Dual Fuzzy-Sugeno Method to Enhance Power Quality Performance using a Single-phase Dual UPQC-Dual PV Without DC-Link Capacitor

Amirullah Amirullah and Adiananda Adiananda

***Abstract*— Unified power quality conditioner (UPQC) is a power electronics device consisting of a series active filter (Se-AF) and a shunt active filter (Sh-AF) connected in parallel through a DC-link circuit to overcome power quality problems, i.e., voltage sag, voltage swell, and non-linear (NL) load. The weakness of the UPQC is that it cannot function normally if the Se-AF and/or Sh-AF fail, and the devices are unable to transfer active power to the load in the event of an interrupt voltage at the source. This paper proposes a novel configuration of a dual UPQC supplied by a dual photovoltaic (PV), hereinafter referred to as 2UPQC-2PV, to improve the power quality performance of a single-phase 220 V/50 Hz distribution system. The 2UPQC-2PV configuration is proposed to anticipate the possible failure of both inverters in one of the UPQC circuits. The PV array replaces the DC-link capacitor to maintain its voltage connected to the DC-link of the UPQC constant while at the same time supplying active power to the load during an interruption voltage. The dual-fuzzy Sugeno (dual-FS) method is used to overcome the weakness of the dual-proportional-integral (dual-PI) control in determining the optimum parameters of proportional and integral constants. There are three disturbances simulated in each-of 2UPQC-2PV and 1UPQC-1PV using dual-FS and dual-PI, i.e., Case 1 (S-Sag-NL), Case 2 (S-Swell-NL), and Case 3 (S -Inter-NL). Each UPQC-PV combination using FS control is compared with PI control resulting in a total of six cases. The 2UPQC-2PV configuration with dual-PI and dual-FS controls, in the three fault cases, is able to produce higher voltage changes than the 1UPQC-1PV configuration. For the 2UPQC-2PV configuration in the three fault cases, Dual-FS control is able to produce lower THDs of load voltage and source current, than the dual-PI control, while meetings the limits of IEEE 519 Standard. In Case 3, the configuration of 2UPQC-2PV using the dual-FS method, is capable of delivering the active power of the load close to that in Case 1.**

***Index Terms*— Dual-fuzzy Sugeno, dual-proportional-integral, power quality, single-phase 2UPQC-2PV, total harmonics distortion.**

NOMENCLATURE

A. Abbreviations

UPQC	unified power quality conditioner
PI	proportional integral
FS	fuzzy Sugeno
FM	fuzzy mamdani
THD	total harmonics distortion
3P3W	three-phase three-wire
3P4W	three-phase four-wire
Se-AF	series active filter
Sh-AF	shunt active filter
PV	photovoltaic
WT	wind turbine
WE	wind energy
BES	battery energy storage
DVR	dynamic voltage control restorer
DSTATCOM	dynamic static compensator
ESS	energy storage system
MPPT	maximum power point tracking
ANN	artificial neural network
STF	self-tuning filter
UVTG	unit vector generator technique
SRF-PLL	synchronous reference frame-phase locked loop
DG	distributed generation
VSC	voltage source converter
FIS	fuzzy inference system
PCC	point common coupling
S-Sag-NL	sinusoidal-sag-non-linear load
S-Swell-NL	sinusoidal-swell-non-linear load
S-Inter-NL	sinusoidal-interruption-non-linear load
2UPQC-2PV	dual UPQC-dual PV
1UPQC-1PV	single UPQC-single PV
MF	membership function
MOSFET	metal oxide semiconductor field effect transistor
IGBT	insulated gate bipolar transistor

Received: February 14, 2023
Accepted: October 23, 2023
Published Online: January 1, 2024
Amirullah Amirullah (corresponding author) is with the Department of Electrical Engineering, Universitas Bhayangkara Surabaya, Surabaya, 60231, Indonesia (e-mail: amirullah@ubhara.ac.id).
DOI: 10.23919/PCMP.2023.000107

THD V_S	THD of source voltage
THD V_{SE}	THD of series compensation voltage
THD V_L	THD of load voltage
THD I_S	THD of source current
THD I_{SH}	THD of shunt compensation current
THD I_L	THD of load current

B. Variables

K_P	proportional constant
K_I	integral constant
L_S	line inductance
L_{SH}	shunt inductance
L_{SE}	series inductance
I_L	load current
I_S	source current
I_{SH}	shunt compensation current
V_L	load voltage
V_S	source voltage
V_{SE}	series compensation voltage
V_{PV}	PV voltage
I_{PV}	PV current
P_{PV}	PV power
V_{DC}	DC-link voltage
P_{DC}	DC-link power
P_L	load active power
i_a, i_b, i_c	load currents for phase "a", "b", and "c"
v_a, v_b, v_c	load voltages for phase "a", "b", and "c"
i_α, i_β, i_o	reference currents for phase "α", "β" and "o"
v_α, v_β, v_o	reference voltages for phase "α", "β" and "o"
p	active power
q	reactive power
$\bar{p}$	average active power
$\bar{q}$	average reactive power
$\tilde{p}$	oscillating active power
$\tilde{q}$	oscillating reactive power
$\bar{p}_{loss}$	instantaneous power loss
$i^*_{\alpha\beta}$	α-β reference current
i^*_{abc}	three phase reference current
V_{DC_crror}	error DC-link voltage
ΔV_{DC_crror}	delta error DC-link voltage
I_C	compensation current
V_{DC}	DC-link voltage
V_{PV}	PV voltage
P_{Load}	load active power
Q_{Source}	source reactive power
Q_{ShAF}	Sh-AF reactive power

I. Introduction

In addition to electricity production, photovoltaic (PV) generators also cause harmonics, and voltage/current disturbances. Because of PV integration, the presence of converters, and the increase in the quantity and capacity of non-linear loads, the power quality of the power system is reduced. A unified power quality conditioner (UPQC), which corrects for power quality issues from the source voltage and/or load current side, can be employed to counteract these disruptions. Series filters and shunt filters are coupled in parallel to form the UPQC. This can provide improved control for many power quality issues [1], [2]. A dual UPQC supply can be created to cater for the breakdown of both inverters in one UPQC circuit. Because such a system can continue to operate even if one of the inverters has a disruption, it is more reliable with better control of the inverter circuit. In this set-up, the voltage and current are controlled by a two-phase, two-stage inverter at the synchronous rotating reference frame [3]. The dual or interline UPQC used to lessen harmonics and voltage/current imbalances consists of two active filters, i.e. a series active filter (Se-AF) and a shunt active filter (Sh-AF) connected in parallel.

Many papers have discussed the deployment of dual UPQC circuits and control to enhance the power quality of supply and load of the low-voltage distribution network. The sinusoidal reference synchronization theory was used to build a straightforward UPQC control approach in the ABC reference frame in [4], whereas in [5], two distinct controls were compared to produce a pulse width modulation (PWM) reference signal using the α-β and d-q reference frames, respectively. There have already been simulations [6], [7] and lab tests [8] comparing the operating performance of single UPQC and dual UPQC in a three-phase three-wire (3P3W) system under static and dynamic faults as well as providing additional adjustment to the grid voltage. Dual UPQC was able to produce better static and dynamic performance than single UPQC, according to the simulation and experimental data.

Under conditions of abrupt load changes, improved power quality using dual UPQC has been investigated in [9], whereas dual UPQC models coupled to 3P3W or three-phase four-wire (3P4W) and 3P4W distribution systems were studied, analyzed, and put into practice utilizing proportional-integral (PI) control in [10], [11]. Power angle control was used to analyze the reactive power balance between Se-AF and Sh-AF on dual

UPQC [12], [13]. The simulation results showed that the proposed method was able to equalize the power processed by each dual UPQC converter under abnormal conditions. A UPQC interline model was developed in [14]–[16] using the configuration of improving interline UPQC, a combination of dynamic voltage control restorer (DVR) and dynamic static compensator (DSTATCOM), and fuzzy logic control, respectively.

A three-phase UPQC configuration using three-dimensional space vector pulse width modulation (3Ph-UPQC-3D-SVPWM) was implemented in [17], while [18] investigated single-phase UPQC using a notch filter and feedback to suppress DC-link voltage ripple due to low frequency effects. In [19], a three-phase-UPQC-modular multilevel converter was implemented to mitigate PQ voltage sources and load currents, while [20] carried out a power flow analysis and increased PQ on the three -phase-UPQC-photovoltaic-wind turbine (3Ph-UPQC-PV-WT) system. A module for an AC microgrid (ACMG) as a three-phase modulated-unified power quality conditioner (3Ph-Modulated-UPQC) was proposed in [21], and a combination of 3Ph-UPQC-PV-WT connected to the 3P3W grid system to increase PQ was examined in [22].

The increase in power in PV and wind energy (PV-WE) systems connected to the UPQC network integrated with energy storage systems (ESS) and electric vehicles (EV) was studied in depth in [23]. The results of the analysis showed that the power output of maximum power point tracking (MPPT)-PV based on fuzzy logic was better than MPPT based on Artificial Neural Networks. Three-phase UPQC to mitigate power quality problems in grid systems and harmonics due to non-linear loads supported by PV and battery energy storage battery energy storage (BES) systems was observed in [24], in which the UPQC control synchronization operation used a self-tuning filter (STF) integrated with the unit vector generator (UVG) technique. This method was able to provide better control over the quality of the load voltage at an unbalanced and distorted source voltage than the synchronous reference frame-phase locked loop (SRF-PLL) method. The DG system that integrates PV with a single-phase system into a three-phase UPQC (DG-UPQC-1Ph-3Ph) was studied in [25], in which the PV generator was capable of injecting power into the grid, serving local loads connected to a 3P3W system, and serving rural and/or remote area customers supplied by a single-phase grid. In [17]–[25], the analyses were performed in the conditions of distorted voltage source, sag/swell voltage, unbalanced voltage, and unbalanced currents due to non-linear loads. A single UPQC-PV system linked to a 3P3W system was also proposed in [26] to reduce voltage sag as well as to sustain load voltage and deliver load power from PV due to interruption voltage. However, the system was unable to properly transfer active power to the load because of load voltage drop caused by the interruption voltage.

Several studies have proposed a dual UPQC system supplied by a PV array. This was subsequently referred to as the dual UPQC-PV system. It was to address the malfunction of one of the inverters and the single UPQC-PV system incapacity to address disruptions brought by the interruption voltage. A dual UPQC-PV system coupled to a 3P4W system was modelled with multilayer inverters to lessen voltage sag, load voltage harmonics, and source current harmonics under various solar radiation in [27], while a dual-UPQC system was injected by two PV arrays in [28] using two distinct DC-link circuits and two three-phase voltage source converters (VSC).

The drawback of the system model in [27], [28] was that it only discussed one level of PV array integration and was only used to lessen harmonics, sag/swell voltages, and imbalances brought by non-linear loads. It did not include any implementation to deal with interruptions and to maintain the active load power at a stable level. It is also necessary to find the best proportional (K_{P}) and integral constants (K_{I}), to use for the Sh-AF circuit in the dual UPQC-PV model. On the basis of the dual-PI and dual-FS methods on the 3P3W system, an improvement in load active power flow performance using the 2UPQC-2PV system was noted in [29], [30]. The three-phase 2UPQC-2PV configuration with dual-FS control was able to increase load active power performance and efficiency of the dual-UPQC circuit better than the dual-PI control in the case of an interrupting voltage with a sinusoidal and distorted source.

This paper applies the single-phase dual UPQC model combined with dual PV, hereinafter referred to as single-phase 2UPQC-2PV, using fuzzy logic control (FLC) with Sugeno's fuzzy inference system (FIS) algorithm. In contrast to the two studies in [29], [30], the dual UPQC model was applied to a single-phase 220 V/ 50 Hz distribution network connected to nonlinear loads. Different from UPQC model configurations that have been examined by previous researchers [27]–[30], the proposed UPQC design does not use the DC-link capacitor. Instead, the PV generator is used as a DC voltage source, and supplies load power when the source experiences an interruption while at the same time it keeps the UPQC DC voltage constant. Referring to the problems described above, the main contributions of this paper are:

1) A single-phase dual UPQC model injected by two PV arrays without DC-link capacitor, namely, single-phase 2UPQC-2PV, is designed in order to reduce source current total harmonics distortion (THD), maintain load voltage, reduce load voltage THD, and enhance load active power performance during voltage

interruption on the source bus. The dual UPQC circuit is placed between the load bus and source bus (PCC), which is connected to a 220 V/50 Hz single-phase distribution system. Both PV arrays 1 and 2 are made up of a number of PV panels, each with a maximum power of 12 kW.

2) To determine the best system configuration for preserving load voltage magnitude, reducing load voltage THD, lowering source current THD, and preserving load active power due to voltage disturbance on the source bus, the performance of the 2UPQC-2PV configuration is validated with the single-phase 1UPQC-1PV.

3) Implementation of the dual-FS control method on the Sh-AF in the single-phase 2UPQC-2PV and 1UPQC-1PV circuits, respectively, to overcome the weakness of PI control in determining the proportional (K_P) and integral constants (K_I) in the two proposed models.

4) Validation of dual-FS results with dual-PI control method on 2UPQC-2PV and 1UPQC-1PV of single-phase Sh-AF circuits to determine the best control method to maintain load voltage magnitude, reduce load voltage and source current THDs, and at the same time maintain load active power in a number of fault conditions on the source bus.

The rest of the paper is arranged as follows. Section II presents the proposed method, i.e., single-phase 2UPQC-2PV system model, simulation parameters, dual Se-AF control circuit, dual Sh-AF control circuit, and dual-PI and dual-FS control methods on a single-phase 2UPQC-2PV circuit. Section III presents the results and discussions on the load voltage, series voltage, source current, shunt compensation current, load current, and their corresponding THDs. It further presents the output power of PV1 and PV2, as well as the load active power using the FS method validated by the PI method. Observations of the results are given on the percentage of sag/swell and disconnection voltages in the proposed dual UPQC circuit using the FS and PI methods. Two dual UPQC circuit configurations and three fault cases are presented and the results are verified using Matlab-Simulink simulation. The validation and comparison of the method with previous research are further discussed. The paper is concluded in Section IV.

II. Research Method

A. Proposed Method

In a single-phase low-voltage distribution system, this study aims to enhance the performance of power quality in a dual UPQC system supplied by a PV array using the dual-FS approach. Both PV arrays 1 and 2 consist of a number of PV panels, and each has a maximum PV power of 12 kW. The single-phase UPQC is a combination of a single-phase Se-AF and a single-phase Sh-AF. In this study, the single-phase Se-AF circuit consists of four MOSFET switches (MO_1, MO_2, MO_3 and MO_4) which inject a compensating voltage to the load bus when a sag/swell occurs on the source bus. The single-phase Sh-AF circuit consists of four IGBT switches (IG_1, IG_2, IG_3 and IG_4) that inject harmonic compensation current to the source bus because of the presence of nonlinear load (NL). In the proposed model, the NL is a full-bridge rectifier with diodes (D_1, D_2, D_3 and D_4) connected to a RL DC load.

The two proposed power electronics devices are the 1UPQC-1PV array and the 2UPQC-2PV arrays. To overcome the shortcomings of the 1UPQC-1PV system and maintain the magnitude of the load voltage while simultaneously reducing the load voltage THD and providing the load bus with a more stable active power supply in the event of voltage interruption on the source bus, the 2UPQC-2PV system is proposed. The suggested UPQC circuit does not include a DC-link capacitor, in contrast to other studies. The dual UPQC circuit is connected to the source bus by a low voltage distribution line at 220 V/50 Hz, and is situated between the source and load buses. The FS control is suggested as a solution to the PI control's shortcomings in the setting of the K_P and K_I Fig. 1 further presents the configuration of the 2UPQC-2PV system. The following three cases explain the disturbances on the source bus for a single-phase system using the two dual UPQC systems.

1) Case 1 (S-Sag-NL): The system is connected to a non-linear load (NL) and the sinusoidal source is experiencing a 50% sag voltage disturbance. The sag voltage in a single-phase system is generated by connecting the 220 V/50 Hz source voltage which is in series with the source inductance ($L_S = 0.1$ mH), in parallel with the inductance component ($L_I = 0.1$ mH) using circuit breaker 1 (CB_1) under normally open (NO) condition.

2) Case 2 (S-Swell-NL): The system is connected to an NL and the source is experiencing a 50% swell voltage disturbance. The swell voltage in a single-phase system is generated by connecting the 220 V/50 Hz source voltage which is in series with the source inductance L_S, in parallel with a 110 V/50 Hz voltage source through circuit breaker 2 (CB_2) under NO condition.

3) Case 3 (S-Inter-NL): The system is connected to an NL and the source is experiencing 100% voltage disturbance. The disconnection voltage in a single-phase system is generated by short-circuiting the 220 V/50 Hz source voltage which is connected in series with the source inductance L_S ,through circuit breaker 3 (CB_3) under NO condition.

The total simulation time for the three disturbances is 0.5 s with a fault duration of 0.2 s between 0.15 s to 0.35 s.

In each case, the FS control is used as DC voltage control on the Sh-AF to enhance power quality, and the results are compared with PI control. There are six examples, with PI and FS controls used in each dual UPQC model in each case. The magnitudes of the source and load voltages and the source and load currents, their corresponding THDs, and the real power of the load are the parameters used for the analysis. The percentage of load voltage disturbance and load active power are calculated in each dual UPQC model in order to choose the circuit model that performs the best in terms of preserving load voltage and load active power in the three disturbance cases after all these parameters have been obtained. Figure 1 depicts the proposed concept without a DC-link capacitor circuit using a single-phase 2UPQC-2PV system. The active power flow employing a single-phase 1UPQC-1PV and 2UPQC-2PV combination is shown in Fig. 2, and the research flowchart of the proposed method is illustrated in Fig. 3. Table I displays the simulation parameters for the proposed model.

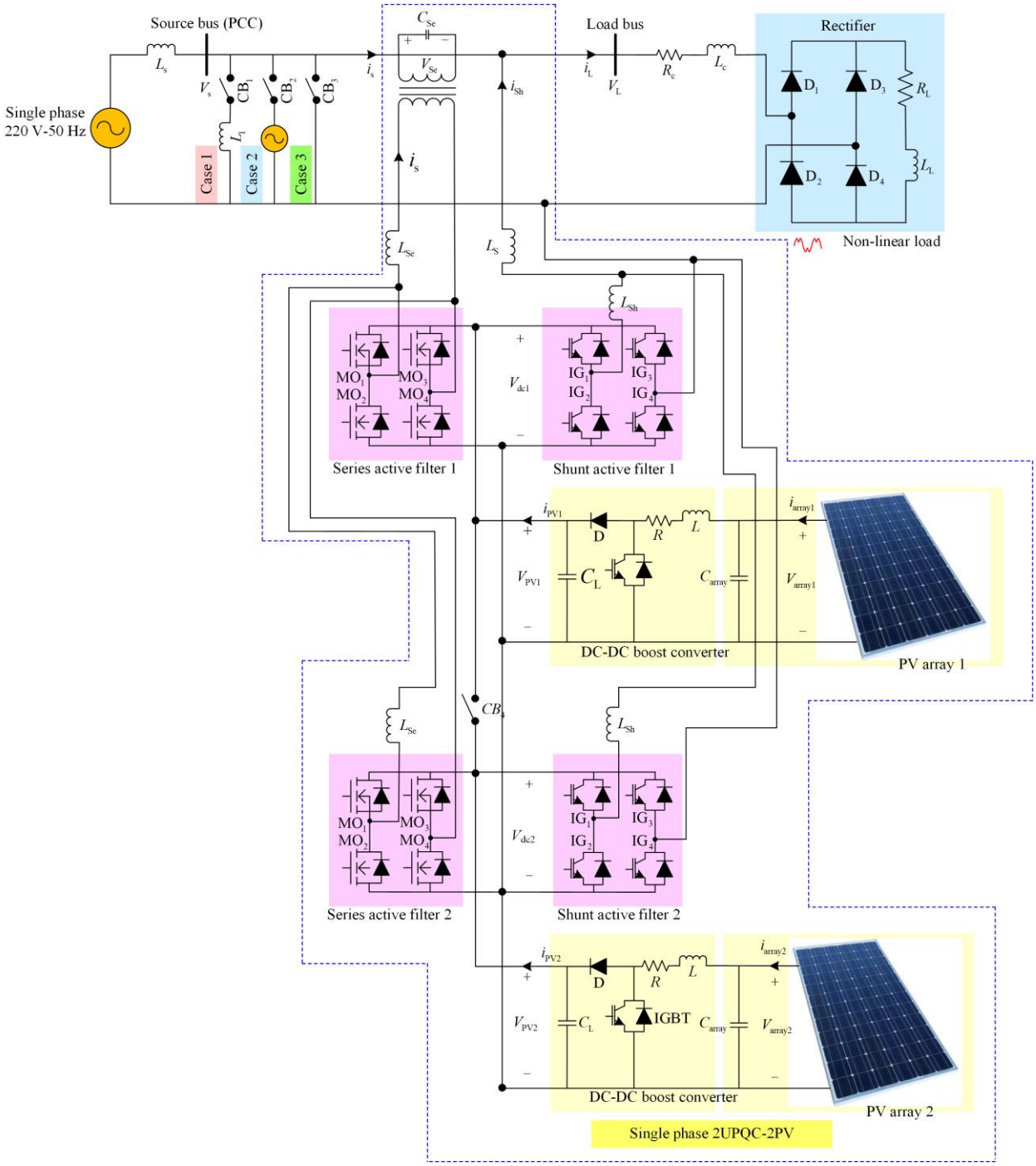

Fig. 1. The proposed model of single-phase 2UPQC-2PV without DC-link capacitor.

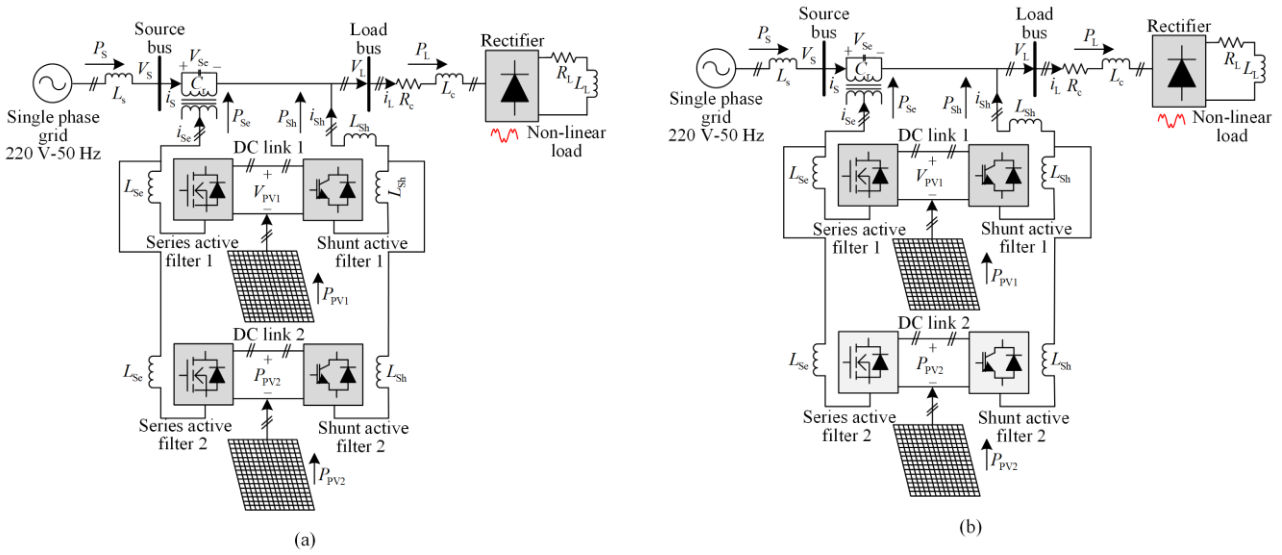

Fig. 2. Active power flow in single-phase. (a) Active power flow in single-phase 1UPQC-1PV. (b) Active power flow in single-phase 2UPQC-2PV.

TABLE I
PARAMETERS OF THE SINGLE-PHASE 2UPQC-2PV SYSTEM

Devices	Parameters	Design values
Single-phase grid	RMS voltage (line-neutral)	220 V
	frequency	50 Hz
	line inductance	$L_S = 0.1$ mH
Sag voltage fault generation (Case 1)	Sag parallel inductance	$L_1 = 0.1$ mH
Swell voltage fault generation	Swell voltage (line-neutral)	110 V
Series-AF	Series inductance	$L_{Se} = 0.001\,5$ mH
Shunt-AF	Shunt inductance	$L_{Sh} = 15$ mH
Series transformer	Rating kVA	1000 kVA
	frequency	50 Hz
	transformation rating (N_1/N_2)	1:1
	series ripple filter	$C_{Se} = 4700$ μF
Non-linear load	Resistance	$R_L = 60\ \Omega$
	inductance	$L_L = 1$ mH
	load impedance	$R_C = 1\ \Omega$ and $L_C = 0.01$ mH
DC-link 1 and 2	DC voltage 1 and 2	$V_{dc} = 100$ V
Photovoltaic array 1 and 2	Active power	12 kW
	irradiance	1000 W/m^2
	temperature	25°C
	MPPT	Perturb and observe
DC-DC converter	Resistanace	$R = 0.01\ \Omega$
	inductance	$L = 0.01$ H
	capacitance	$C_L = 0.002$ F
PI 1 and 2	K_P 1 and 2	$K_P = 0.2$
	K_I 1 and 2	$K_I = 1.5$
Fuzzy logic controller 1 and 2	Fuzzy inference system	Sugeno
	composition	max-min
	defuzzyfication	wtaver
Input memberships function 1 and 2	Error ($V_{dc}(V_{dc\text{-}error})$	Trapmf and trimf
	delta Error $V_{dc}(\Delta V_{dc\text{-}error})$	trapmf and trimf
Output membership function 1 and 2	Instantaneous of power losses $(\bar{p}_{loss})$	constant [0,1]

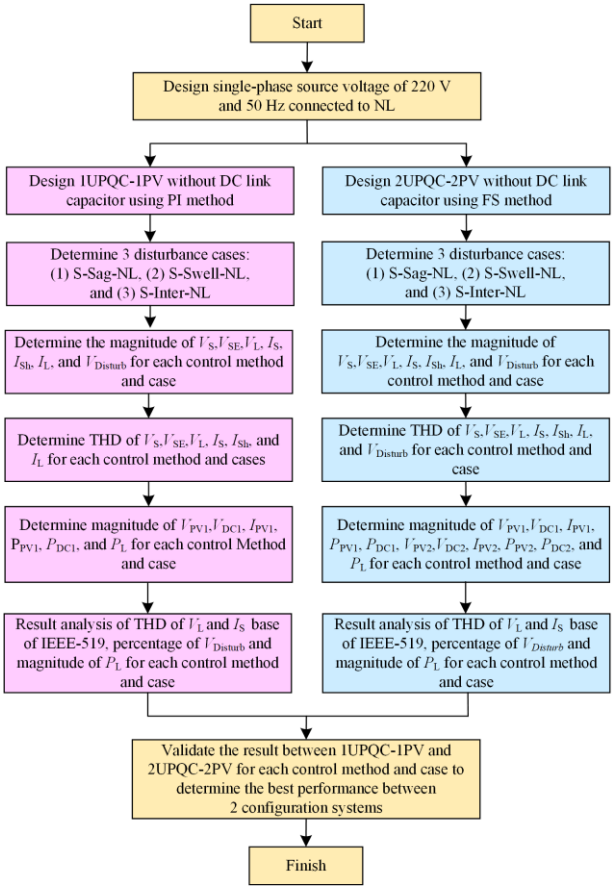

Fig. 3. Research flowchart.

B. Single-Phase Dual Series Active Filter Control

The implementation of Se-AF control on a single UPQC connected to a single-phase system using the unit vector templates generation (UVTG) method can be found in [31]. Based on this circuit model, the Se-AF control circuit in a dual UPQC connected single-phase system is constructed by duplicating a single Se-AF control circuit while still using a single-phase series transformer circuit. Based on this procedure, a complete control of a single-phase dual UPQC is proposed as shown in Fig. 4. The magnitude of the peak fundamental input voltage (V_m) is selected at the nominal voltage of 220 V.

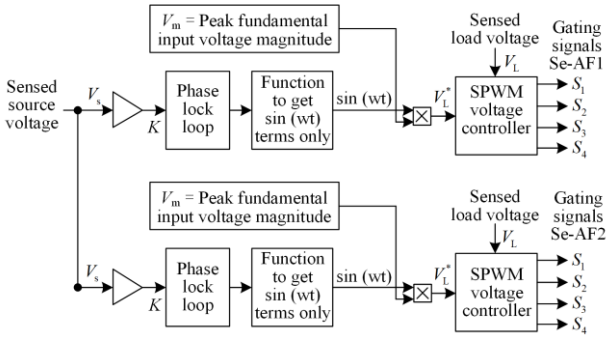

Fig. 4. Control of dual Se-AF on a single-phase system.

C. Single-Phase Dual Shunt Active Filter Control

As a part of the UPQC control, Sh-AF control in a single-phase system has been described in detail in [32]. Based on this circuit model, the Sh-AF control circuit on a dual UPQC is constructed by duplicating the control circuit on a single Sh-AF. For three-wire, three-phase and three-phase four-wire power systems, P-Q theory, often referred to as instantaneous power theory, is normally used. This theory uses three voltage and current signals, but can also be applied to single-phase active filters by duplicating two more voltage and current signals with an angular shift of 120º. The basis of this theory is the division of power components into mean and oscillations. Assigning phase "a" to the load current of the single-phase load, and phases "b" and "c" to the additional phases of the doubling technique, mathematically, the load current i_a can be expressed as phase current "a" using (1) while (2) and (3) can be used to describe the load currents i_b and i_c for phases "b" and "c", respectively as [32]:

$$i_a = \sum_{i=0}^{n} \sqrt{2} I_i \sin(w_i + \theta_i) \tag{1}$$

$$i_b = \sum_{i=0}^{n} \sqrt{2} I_i \sin(w_i + \theta_i - 120°) \tag{2}$$

$$i_c = \sum_{i=0}^{n} \sqrt{2} I_i \sin(w_i + \theta_i - 120°) \tag{3}$$

Where I_i is a single-frequency root mean square current at the *i*th harmonic; w_i is the angular frequency of the waveform in radians per second at the *i*th harmonic; and θ_i is the phase angle in degrees or radians per second at the *i*th harmonic.

Equations (1)–(3) can be converted into a matrix form for the load current and load voltage as [32]:

$$\begin{bmatrix} i_a \\ i_b \\ i_c \end{bmatrix} = \begin{bmatrix} 1 \\ 1\angle 120° \\ 1\angle 240° \end{bmatrix} [i_a] \tag{4}$$

$$\begin{bmatrix} v_a \\ v_b \\ v_c \end{bmatrix} = \begin{bmatrix} 1 \\ 1\angle 120° \\ 1\angle 240° \end{bmatrix} [v_a] \tag{5}$$

where the v_a, v_b and v_c are the load voltage for phases "a", "b" and "c."

The reference load current i_α, i_β and i_o, and reference load voltage v_α, v_β and v_o can be calculated using the Clarke transformation as [32]:

$$\begin{bmatrix} i_\alpha \\ i_\beta \\ i_o \end{bmatrix} = \sqrt{\frac{2}{3}} \begin{bmatrix} 1 & -\frac{1}{2} & \frac{1}{2} \\ 0 & \frac{\sqrt{3}}{2} & -\frac{\sqrt{3}}{2} \\ \frac{1}{\sqrt{2}} & \frac{1}{\sqrt{2}} & \frac{1}{\sqrt{2}} \end{bmatrix} \begin{bmatrix} i_a \\ i_b \\ i_c \end{bmatrix} \tag{6}$$

$$\begin{bmatrix} v_\alpha \\ v_\beta \\ v_o \end{bmatrix} = \sqrt{\frac{2}{3}} \begin{bmatrix} 1 & -\frac{1}{2} & \frac{1}{2} \\ 0 & \frac{\sqrt{3}}{2} & -\frac{\sqrt{3}}{2} \\ \frac{1}{\sqrt{2}} & \frac{1}{\sqrt{2}} & \frac{1}{\sqrt{2}} \end{bmatrix} \begin{bmatrix} v_{\mathrm{a}} \\ v_{\mathrm{b}} \\ v_{\mathrm{c}} \end{bmatrix} \tag{7}$$

According to [32], the active power p and reactive power q can be expressed as:

$$p = v_\alpha i_\alpha + v_\beta i_\beta + v_o i_o \tag{8}$$

$$q = v_\alpha i_\alpha + v_\beta i_\beta \tag{9}$$

$$\begin{bmatrix} p \\ q \end{bmatrix} = \begin{bmatrix} v_\alpha & v_\beta \\ -v_\beta & v_\alpha \end{bmatrix} \begin{bmatrix} i_\alpha \\ i_\beta \end{bmatrix} \tag{10}$$

The two sections that make up the active power and reactive power are the average and oscillating power, or the DC part and AC part, expressed as [32]:

$$p = \bar{p} + \tilde{p} \tag{11}$$

$$q = \bar{q} + \tilde{q} \tag{12}$$

where $\bar{p}$ is average active power; $\bar{q}$ is the average reactive power; $\tilde{p}$ is the oscillating active power; and $\tilde{q}$ is the oscillating reactive power.

A low-pass filter, which removes high frequencies, can be used to determine the DC portion. Equation (13) can be used to describe the reference current α-β ($\boldsymbol{i}^*_{\alpha\beta}$) of the DC active power and reactive power sections [33].

$$\boldsymbol{i}^*_{\alpha\beta} = \frac{1}{v_\alpha^2 + v_\beta^2} \begin{bmatrix} v_\alpha & v_\beta \\ -v_\beta & v_\alpha \end{bmatrix} \begin{bmatrix} -\tilde{p} + \bar{p}_{\mathrm{loss}} \\ -q \end{bmatrix} \tag{13}$$

The average active power is obtained by using theparameter $\bar{p}_{\mathrm{loss}}$ of the voltage controller. This value is in the form of instantaneous active power which corresponds to the resistive loss and switching loss of the UPQC. The three-phase reference current of the active power filter $\boldsymbol{i}^*_{\mathrm{abc}}$ is given in (14) [33]. A PWM signal is generated using a hysteresis band. Only two of the six PWM signals generated are used as the hysteresis band input for the single-phase Sh-AF.

$$\boldsymbol{i}^*_{\mathrm{abc}} = \sqrt{\frac{2}{3}} \begin{bmatrix} 1 & 0 \\ -\frac{1}{2} & \frac{\sqrt{3}}{2} \\ -\frac{1}{2} & -\frac{\sqrt{3}}{2} \end{bmatrix} \boldsymbol{i}^*_{\alpha\beta} \tag{14}$$

To operate properly, dual UPQC must have a minimum DC-link voltage V_{DC} as [24]:

$$V_{\mathrm{DC}} = \frac{2\sqrt{2}V_{\mathrm{Ph-N}}}{\sqrt{3}m} \tag{15}$$

where m is the modulation index; and $V_{\mathrm{Ph-N}}$ is the phase-to-neutral source. Using m of 1 and $V_{\mathrm{Ph-N}}$ of 220 V, V_{DC} is calculated to be 359.26 V, so the value of 400 V is selected.

Based on the duplication of (1)–(14), a dual Shunt-AF control model is further developed on a single-phase system using the dual-FS method shown in Fig. 5.

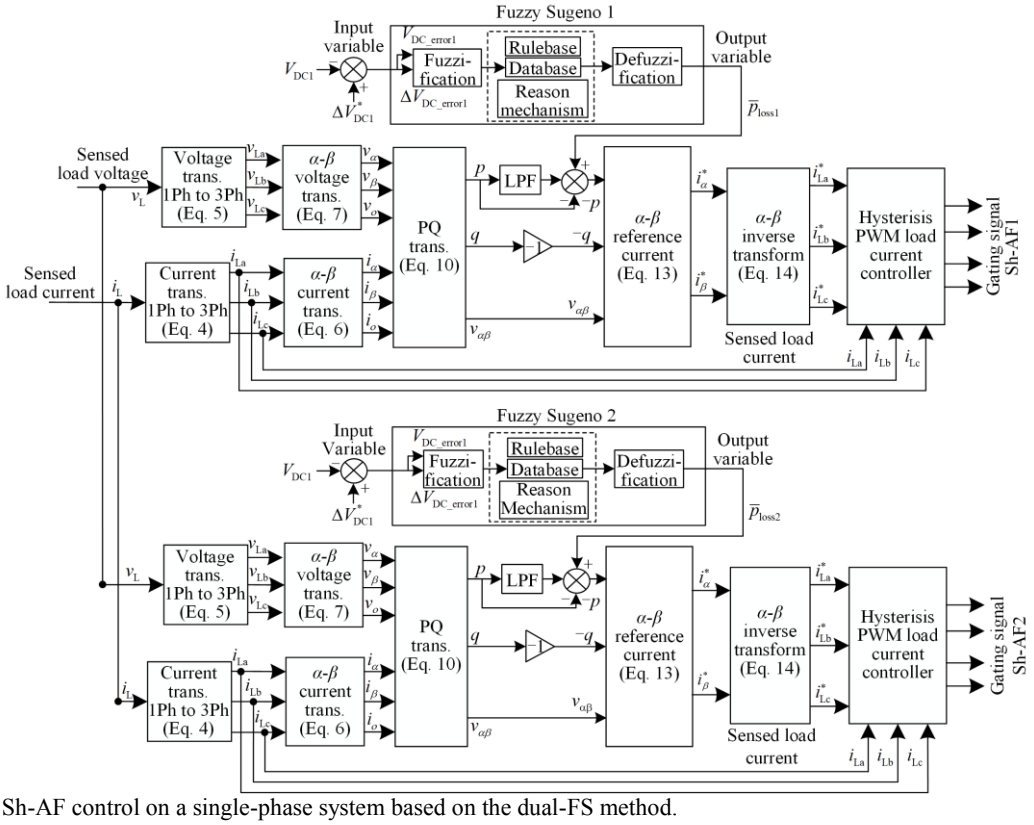

Fig. 5. Dual Sh-AF control on a single-phase system based on the dual-FS method.

D. Design of Dual Fuzzy Sugeno Control

Dual Sh-AF control in the dual UPQC circuit begins by specifying $\bar{p}_{\text{loss}}$ as the input variable to generate a reference source current in the hysteresis current control and a trigger signal in the Sh-AF IGBT circuit from UPQC with PI 1 and PI 2 controls ($K_{\text{P}} = 0.2$ and $K_{\text{I}} = 1.5$). Using the same procedure, $\bar{p}_{\text{loss}}$ is also determined using FS 1 and FS 2. Considerations for choosing FIS with the FS method over the Fuzzy Mamdani (FM) method are because such system uses single membership functions (MFs) which have a membership degree of 1 for a single crisp value and 0 for other crisp values. With this model configuration, FS produces a faster simulation because it has a weighted average to replace the defuzzification phase in FM which requires a relatively long simulation time [34]. FS1 and FS2 consists of fuzzification, decision-making (rulebase, database, reason mechanism), and defuzzification as shown in Fig. 5. FIS on FS1 and FS2 uses the Sugeno Method with max-min for input variables and [0, 1] for output variables. FIS consists of three parts, namely, rulebase, database, and reason-mechanism [35]. The FS 1 and FS 2 methods are applied by determining the input variables, namely, the value of V_{DC} error $V_{\text{DC-error}}$ and delta V_{DC} error $\Delta V_{\text{DC-error}}$ to determine $\bar{p}_{\text{loss}}$ at the defuzzification phase.

The value $\bar{p}_{\text{loss}}$ is the input variable to get the compensation current $(\boldsymbol{i}^{*}_{\alpha\beta})$ in (16). During the fuzzification process, a number of input variables are calculated and converted into linguistic variables called MFs. The values of $V_{\text{DC-error}}$ and $\Delta V_{\text{DC-error}}$ are selected as input variables with $\bar{p}_{\text{loss}}$ as output variables. The values of the two input variables and one output variable on the MFs are divided into seven linguistic variables, respectively. The crips input variables used in $V_{\text{DC-error}}$ and $\Delta V_{\text{DC-error}}$ are negative big (NB), negative medium (NS), negative small (NM), zero (Z), positive small (PS), positive medium (PM) and positive big (PB). Crips input variables are triangular and trapezoidal membership functions with limits between −400 and 400. Crips output is $\bar{p}_{\text{loss}}$ in the form of two different constant values [0, 1] with membership function limits between −100 to 100 on FS1 and FS2, respectively. The crips input and output variables have the same linguistic variables. Membership Function (MF) input $V_{\text{DC−error}}$ and $\Delta V_{\text{DC−error}}$ and MF output $\bar{p}_{\text{loss}}$ of FS 1 and FS 2 are presented in Figs 6–8, respectively. Tables II–IV show the linguistic functions and boundaries of the FS 1 and FS 2 set of MF input $V_{\text{DC−error}}$ and $\Delta V_{\text{DC−error}}$ and MF output $\bar{p}_{\text{loss}}$, respectively.

After $V_{\text{DC−error}}$ and $\Delta V_{\text{DC−error}}$ are obtained, the next two MF inputs are converted into linguistic variables and used as input functions for FS 1 and FS 2. Table V presents the MF output generated using the inference block and rules base of FS 1 and FS 2. Then, the defuzzification block finally operates to convert the resulting $\bar{p}_{\text{loss1}}$ and $\bar{p}_{\text{loss2}}$ outputs from the linguistic variables back to numeric variables. $\bar{p}_{\text{loss1}}$ and $\bar{p}_{\text{loss2}}$ then become input variables for current hysteresis control to generate trigger signals for IGBT 1 and IGBT 2 on the Sh-AF dual UPQC circuits to reduce source current harmonics. At the same time, they also improved the power quality of the single-phase system of the three fault cases in the two proposed UPQC configurations of 1UPQC-1PV and 2UPQC-2PV, respectively.

TABLE II
LINGUISTIC FUNCTIONS AND BOUNDARIES OF THE FS 1 AND FS 2 SET OF INPUT VARIABLES OF $V_{\text{DC−error}}$

No.	Input variables	Linguistic functions	MFs	Boundaries parameter
1	Negative big	NB	trapmf	−400, −240, −120
2	Negative medium	NM	trimf	−240, −120, −40
3	Negative small	NS	trimf	−120, −40, 0
4	Zero	Z	trimf	−40, 0, 40
5	Positive small	PS	trimf	0, 40, 120
6	Positive medium	PM	trimf	40, 120, 240
7	Positive big	PB	trapmf	120, 240, 400

TABLE III
LINGUISTIC FUNCTIONS AND BOUNDARIES OF THE FS 1 AND FS 2 SET OF INPUT VARIABLES OF $\Delta V_{\text{DC−error}}$

No.	Input variables	Linguistic functions	MFs	Boundaries parameter
1	Negative big	NB	trapmf	−400, −300, −200
2	Negative medium	NM	trimf	−300, −200, −100
3	Negative small	NS	trimf	−200, −100, 0
4	Zero	Z	trimf	−100, 0, 100
5	Positive small	PS	trimf	0, 100, 200
6	Positive medium	PM	trimf	100, 200, 300
7	Positive big	PB	trapmf	200, 300, 400

TABLE IV
LINGUISTIC FUNCTIONS AND BOUNDARIES OF THE FS 1 AND FS 2 OF OUTPUT VARIABLES OF $\bar{p}_{\text{loss}}$

No.	Output variables	Linguistic functions	MFs	Boundaries parameter
1	Negative big	NB	constant [0,1]	−100
2	Negative medium	NM	constant [0,1]	−60
3	Negative small	NS	constant [0,1]	−30
4	Zero	Z	constant [0,1]	0
5	Positive small	PS	constant [0,1]	30
6	Positive medium	PM	constant [0,1]	60
7	Positive Big	PB	constant [0,1]	100

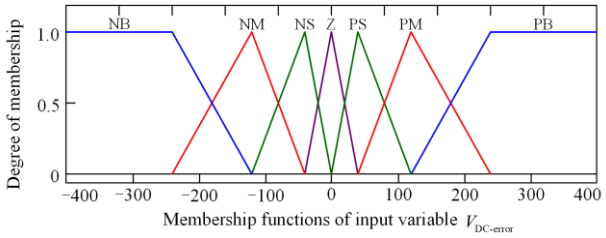

Fig. 6. Input MFs of $V_{\text{DC-error}}$.

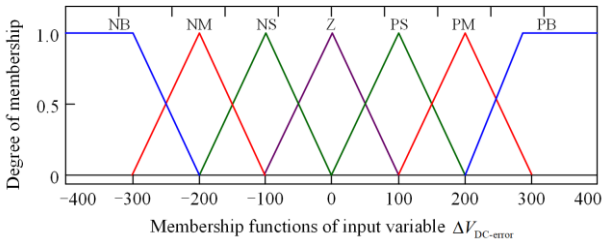

Fig. 7. Input MFs of $\Delta V_{\text{DC-error}}$.

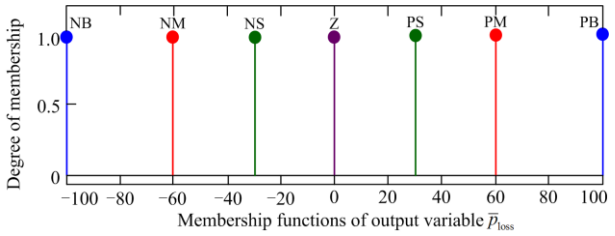

Fig. 8. Output MFs of $\bar{p}_{\text{loss}}$.

TABLE V
FUZZY RULE BASE OF FS 1 AND FS 2

$V_{\text{DC-error}}$ / $\Delta V_{\text{DC-error}}$	NB	NM	NS	Z	PS	PM	PB
PB	Z	PS	PS	PM	PM	PB	PB
PM	NS	Z	PS	PS	PM	PM	PB
PS	NS	NS	Z	PS	PS	PM	PM
Z	NM	NS	NS	Z	PS	PS	PM
NS	NM	NM	NS	NS	Z	PS	PS
NM	NB	NM	NM	NS	NS	Z	PS
NB	NB	NB	NM	NM	NS	NS	Z

E. Percentage Sag/Swell and Interruption Voltage

The sag/swell and interruption voltage monitoring was in accordance to IEEE 1159–1995. This regulation provides a table of definitions of sag/swell and different fault voltages by category (momentary and transient) considering the typical duration and magnitude. Then, the percentage of disturbance of sag/swell and interruption voltage D is proposed as:

$$D = \frac{\left|V_{\text{pre\_disturb}} - V_{\text{disturb}}\right|}{V_{\text{pre\_disturb}}} \times 100\% \quad (16)$$

where $V_{\text{pre\_disturb}}$ is the load voltage before disturbance of sag/swell and interruption voltage happens and is selected as 220 V for all cases; V_{disturb} is the load voltage after disturbance of sag/swell and interruption voltage happens and its value is different for each case.

III. RESULT AND DISCUSSION

A. Simulation Results

The proposed model uses two UPQC-PV combinations connected to a single-phase (on-grid) system via a DC link circuit without a capacitor. Two UPQC-PV combinations are proposed, namely 1UPQC-1PV and 2UPQC-2PV. A single-phase CB is used to connect and disconnect the second UPQC-PV circuit to the first UPQC-PV circuit. The disturbance simulation is the combinations of 1UPQC-1PV and 2UPQC-2PV, with each consisting of three cases, i.e., Case 1 (S-Sag-NL), Case 2 (S-Swell-NL), and Case 3 (S-Inter-NL). Each UPQC-PV combination uses FS control and is validated by PI control thus resulting in a total of six cases.

By using Matlab Simulink, each model combination is executed according to the proposed case to obtain the waveforms of the source voltage (V_{S}), series voltage (V_{SE}), load voltage (V_{L}), source current (I_{S}), shunt current (I_{SH}), and load current (I_{L}). Based on the waveforms, their magnitudes and corresponding THDs are obtained. The measurement of the magnitude of the voltage, nominal current, and THD values in each UPQC-PV combination was carried out in 3 cycles between 0.22 s–0.28 s. The next process performs simulations on a number of proposed cases to obtain curves and determine the values of PV voltage (V_{PV}), PV current (I_{PV}), and PV power (P_{PV}), and their contribution to changes in load active power (P_{L}), which are carried out in one cycle at 0.25 s. The PV power value is measured after the DC-DC boost converter circuit so its value is the same as the DC-link power because the UPQC circuit does not use capacitors. The total simulation time for disturbances in Cases 1–3 is 0.5 s with a disturbance duration of 0.2 s between 0.15 s–0.35 s.

Figure 9 presents the performance of V_S, V_{SE}, V_L, I_S, I_{SH} and I_L for 2UPQC-2PV and dual-FS control in Case 1 (S-Sag-NL). It shows that in the configuration and control method at 0.15 s to 0.35 s from the total simulation duration of 0.5 s, the source voltage V_S decreases by 50% from 220 V to 113.4 V. In this condition, voltages DC1 (V_{DC1}) and DC2 (V_{DC2}) are not able to produce maximum power and only inject a series compensation voltage (V_{SE}) of 102.9 V through the series transformer on the Se-AF. Thus, in the Case 1 period, the load voltage V_L on the single-phase system decreases slightly to 216.3 V. The decrease in the V_L eventually also causes the I_L to slightly decrease to 3515 A. On the other hand, in the same case, the 2UPQC-2PV configuration is able to inject a shunt compensation current I_{SH} of 15.11 A and a THD of0.34% with the opposite phase direction so as to reduce the THD of the source current I_S to 0.47% compared to I_L THD of 1.68%.

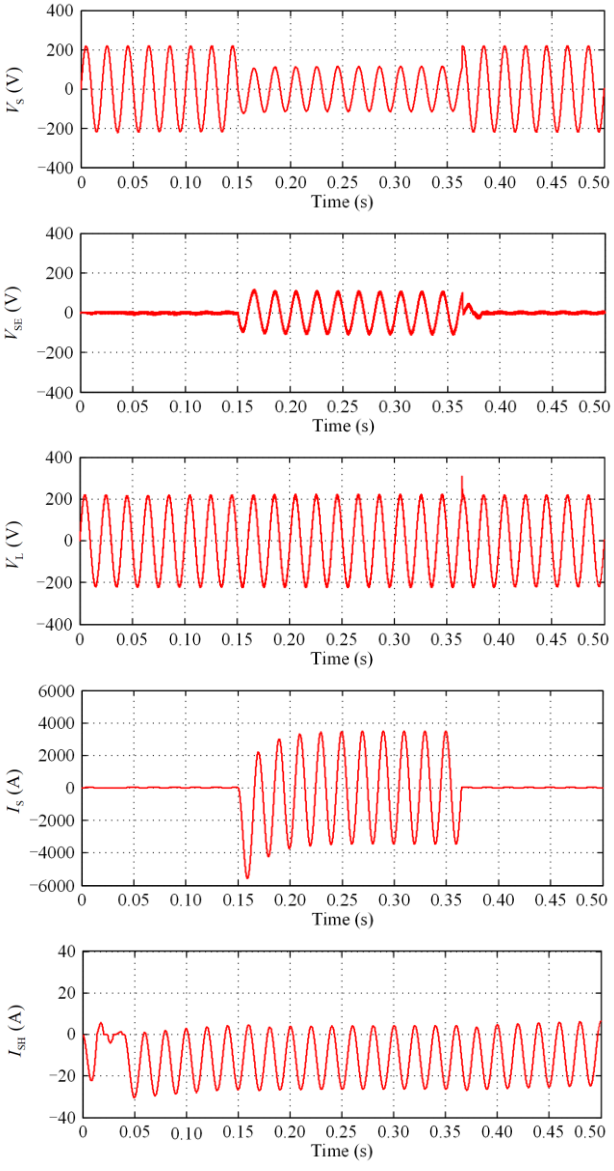

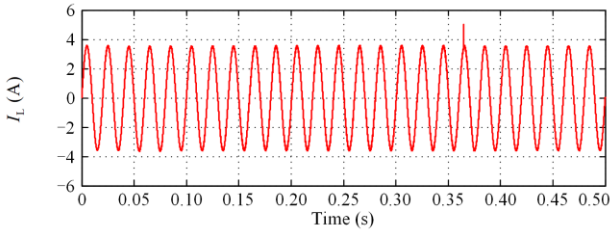

Fig. 9. Performance of V_S, V_{SE}, V_L, I_S, I_{SH} and I_L from 2UPQC-2PV using dual-FS control in Case 1 (S-Sag-NL).

In the same case, and same configuration and control method, Fig. 10 shows that because the system does not use a DC-link capacitor, DC1 voltage (V_{DC1}) and DC2 voltage (V_{DC2}) are the same as PV1 voltage (V_{PV1}) and PV2 voltage (V_{PV2}) of 176.4 V. The PV1 and PV2 generators generate the same PV1 power (P_{PV1}) and PV2 power (V_{PV2}) of 72,750 kW with PV1 current I_{PV1} and PV2 current I_{PV2} of 530.9 A. Figure 10 also shows that the nominal PV1 power (P_{PV1}) and PV2 power (P_{PV2}) are equal to DC1 power (P_{DC1}) and DC2 power (P_{DC2}), while delivering 380.3 W load active power (P_L).

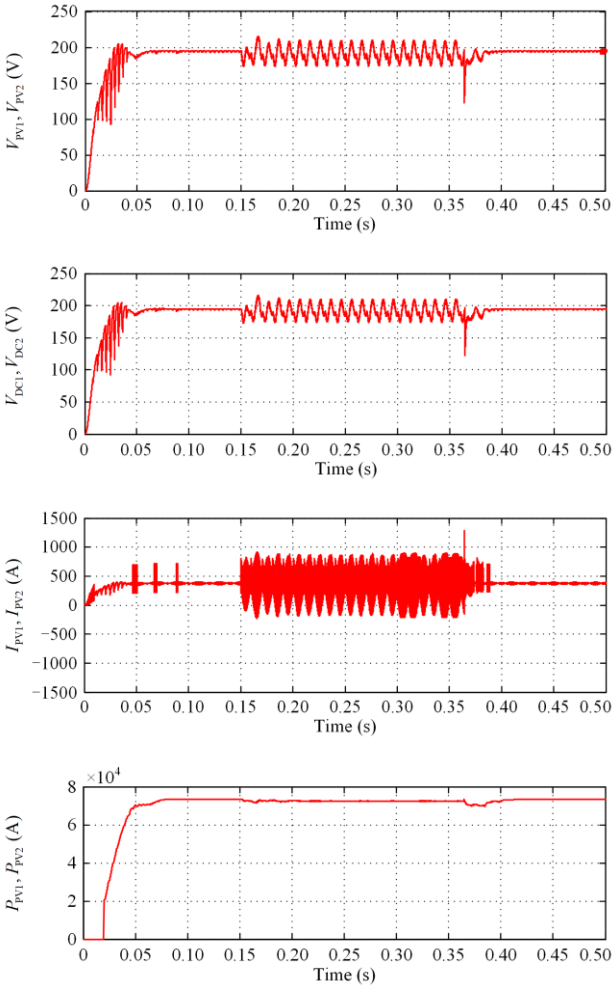

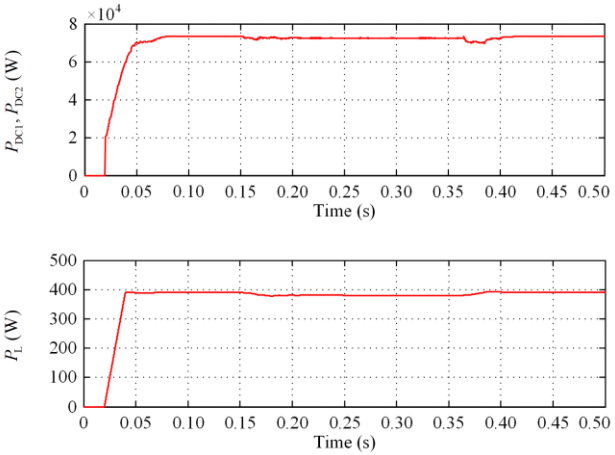

Fig. 10. Performance of V_{PV}, V_{DC}, I_{PV}, P_{PV}, P_{DC} and P_L from 2UPQC-2PV using dual-FS control in Case 1 (S-Sag-NL).

Figure 11 shows the performance of V_S, V_{SE}, V_L, I_S, I_{SH} and I_L in the 2UPQC-2PV configuration connected to a single-phase system using dual-FS control in Case 2 (S-Swell-NL), while Fig. 12 shows the performance of V_{PV}, V_{DC}, I_{PV}, P_{PV}, P_{DC} and P_L.

Figure 11 shows that in the configuration and control method during 0.15 s to 0.35 s, the V_S increases 50% from 220 V to 321 V. In this condition, PV1 and PV2

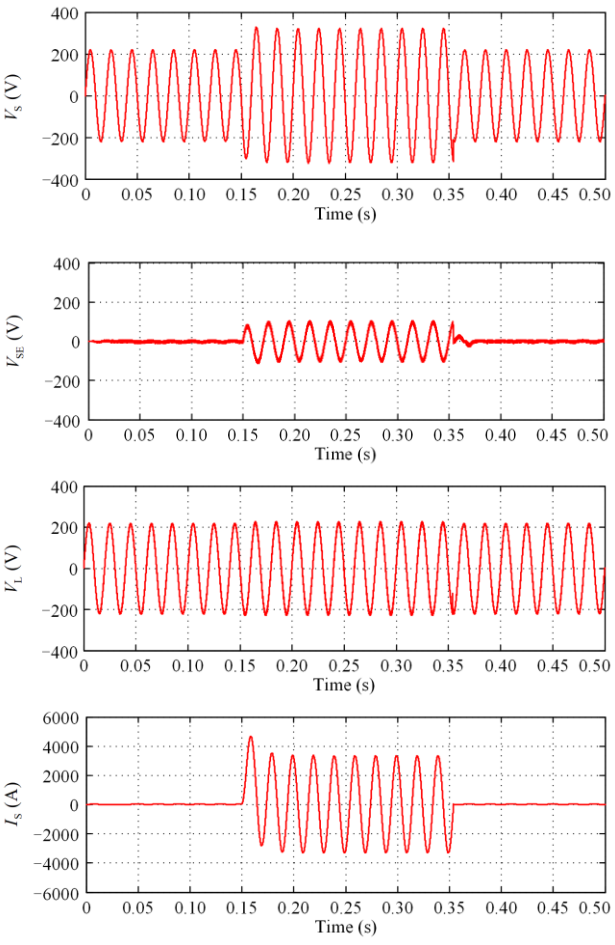

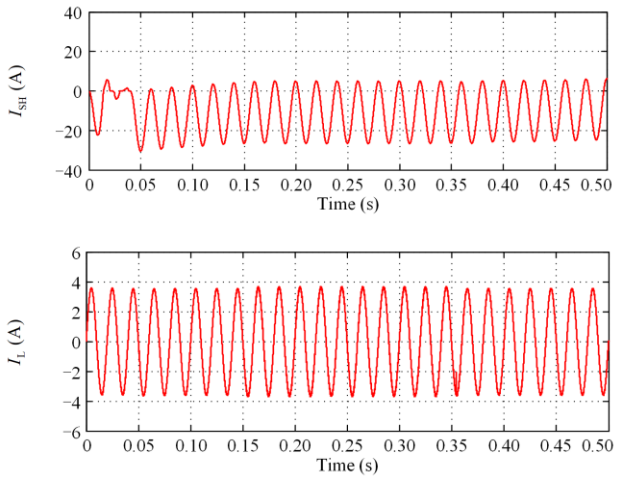

Fig. 11. Performance of V_S, V_{SE}, V_L, I_S, I_{SH} and I_L for configuration 2UPQC-2PV using dual-FS control in Case 2 (S-Swell-NL).

are able to maintain V_{DC1} and V_{DC2} so that they can inject a V_{SE} with an opposite phase of 97.4 V through a series transformer on the Se-AF. Thus, in Case 1, the V_L in the single-phase system increases slightly to 223.7 V. The increase in the V_L eventually also causes the load current I_L to slightly increase to 3634 A. On the other hand, in Case 2, the 2UPQC-2PV configuration is able to inject the shunt compensation current I_{SH} with the opposite phase direction of 15.83 A and THD of 0.23%, and reduce the THD of I_S to 0.01% compared to the I_L THD of 1.19%.

For the same Case 2, and same configuration and control method, Fig. 12 shows that the V_{DC1} and V_{DC2} are the same as the V_{PV1} and V_{PV2} of 171.6 V. PV1 and PV2 generate the same P_{PV1} and P_{PV2} of 72.41 kW with I_{PV1} and I_{PV2} of 454.3 A. Figure 12 also shows that the P_{PV1} and P_{PV2} are equal to the P_{DC1} and P_{DC2} delivering the P_L of 406.2 W.

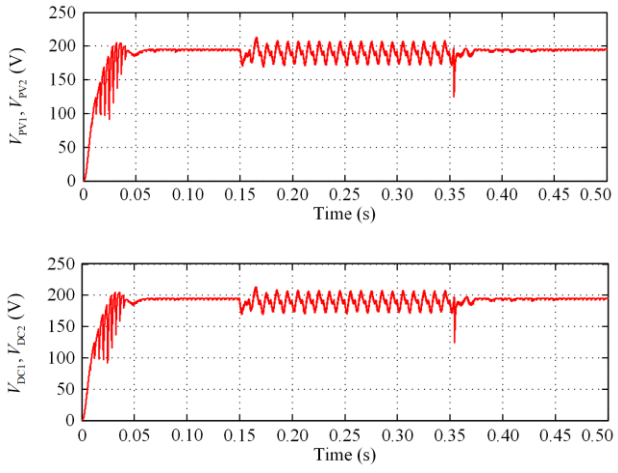

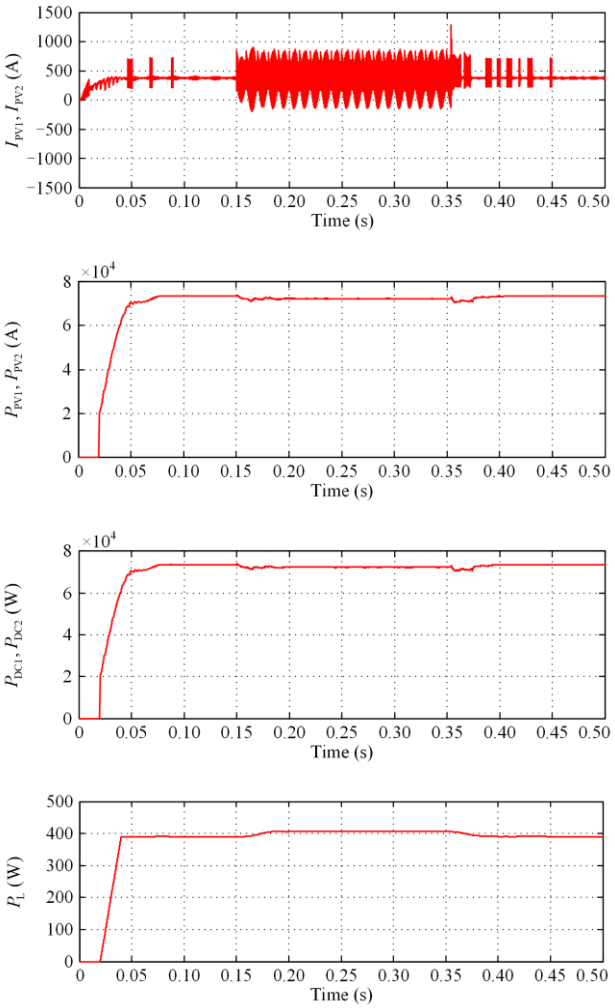

Fig. 12. Performance of V_{PV}, V_{DC}, I_{PV}, P_{PV}, P_{DC} and P_L for configuration 2UPQC-2PV using dual-FS control in Case 2 (S-Swell-NL).

Figure 13 shows the performance of V_S, V_{SE}, V_L, I_S, I_{SH} and I_L in the 2UPQC-2PV configuration connected to a single-phase system using dual-FS control in Case 3 (S-Inter-NL) conditions, while Fig. 14 shows the performance of $V_{PV}, V_{DC}, I_{PV}, P_{PV}, P_{DC}$ and P_L.

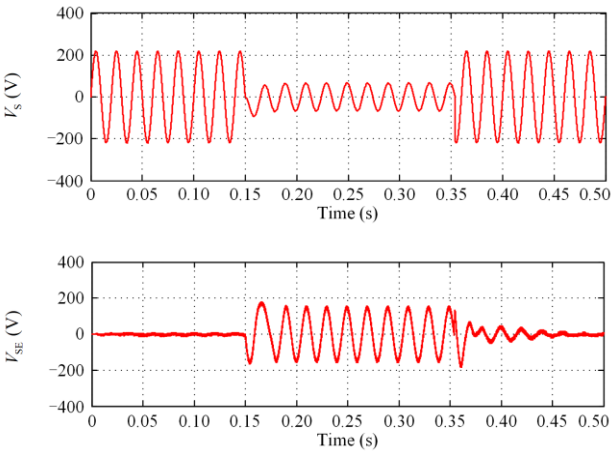

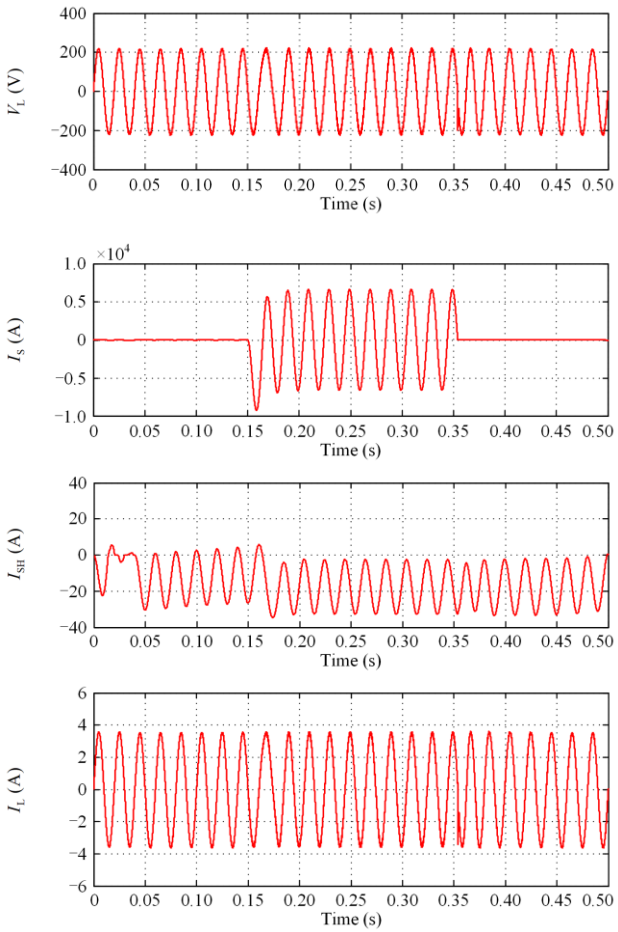

Fig. 13 Performance of V_S, V_{SE}, V_L, I_S, I_{SH} and I_L for configuration of 2UPQC-2PV using dual-FS control in Case 3 (S-Inter-NL)

Figure 13 shows that in this configuration and control method, the V_S drops from 220 V to 66.6 V. In this condition, PV1 and PV2 are able to maintain the V_{DC1} and V_{DC2} so that it can inject a V_{SE} with an opposite phase of 149.8 V through the Se-AF series transformer. Thus, in Case 3, the V_L on the single-phase system slightly decreases to 216.2 V. A small decrease in the V_L eventually also causes the I_L to slightly decreases to 3512 A. On the other hand, in Case 3, the 2UPQC-2PV configuration is able to inject I_{SH} through the Sh-AF with the opposite phase direction of 15.11 A and THD of 2.98%, so as to reduce the THD of the I_S to 0.01% compared to the l I_L THD of 2.65%.

In the same case, and with the same configuration and control method, Fig. 14 shows that because the system

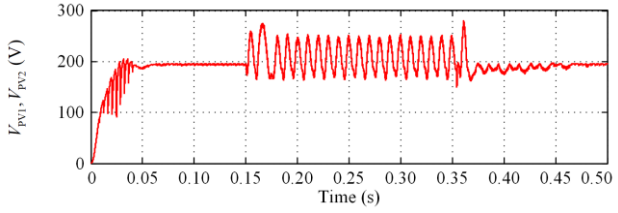

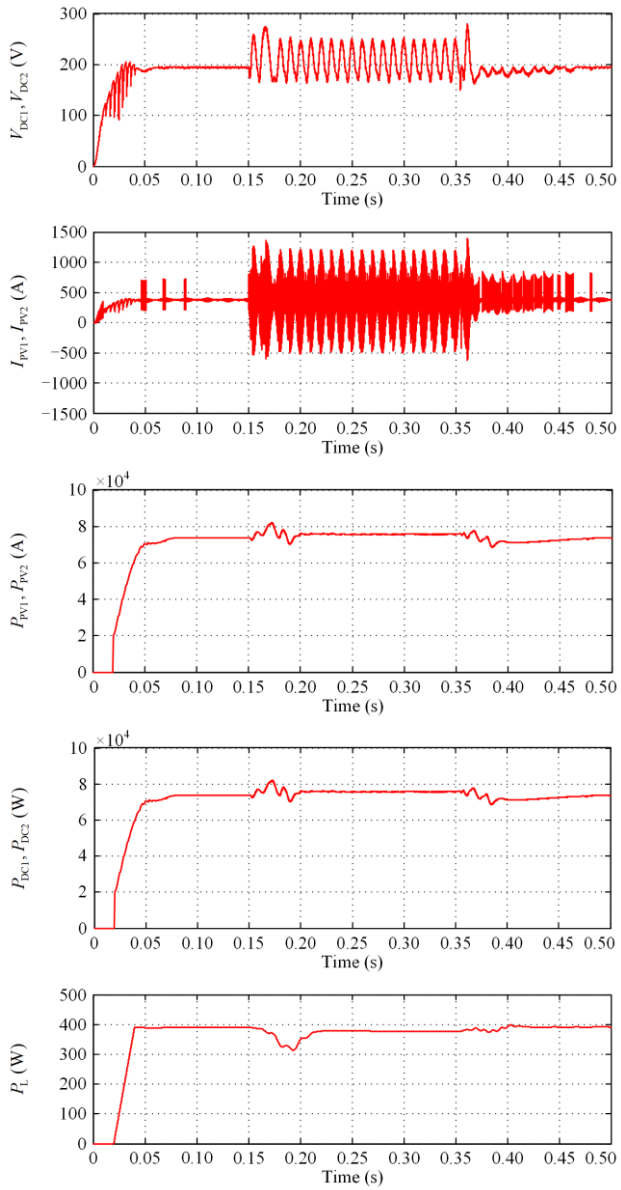

Fig. 14 Performance of V_{PV}, V_{DC}, I_{PV}, P_{PV}, P_{DC} and P_L for configuration of 2UPQC-2PV using dual-FS control in Case 3 (S-Inter-NL)

does not use a DC-link capacitor, the V_{DC1} and V_{DC2} are equal to the V_{PV1} and V_{PV2} of 203.7 V. PV1 and PV2 generate the same P_{PV1} and P_{PV2} of 75.79 kW with I_{PV1} and I_{PV2} of 562.9 A. Figure 14 also shows that the nominal output power of P_{PV1} and P_{PV2} are equal to P_{DC1} and P_{DC2}, while delivering a P_L of 378.6 W.

B. Analysis of Voltage Magnitude, Current, and Load Voltage Change

Using the same procedure, the magnitudes of $V_S, V_{SE}, V_L, I_S, I_{SH}$ I_L and $V_{Disturb}$ using (16), as well as their respective THD values and the values of $V_{PV}, V_{DC}, I_{PV}, P_{PV}, P_{DC}$ and P_L in different cases and configurations of UPQC-PV using the PI and FS control methods are presented in more detail in Tables VI–XI.

Table VI shows that in Cases 1–3, a single-phase system using 1UPQC-1PV with PI control is able to maintain a V_L of 218.6 V, 221.8 V, and 218.3 V, respectively. In the same configuration and using FS control, Cases 1-3 are able to maintain similar V_L of 218.1 V, 221.8 V, and 218.5 V, respectively. Table VI also shows that in Cases 1–3, a single-phase system using 1UPQC-1PV with PI control is still capable of carrying I_L of 3.543 A, 3.604 A, and 3.546 A, respectively. With FS control, Cases 1 are also capable of carrying similar I_L of 3.543 A, 3.605 A, and 3.550 A, respectively. Table VI also shows that in Cases 1–3, a single-phase system using 1UPQC-1PV with PI control produces respectively load voltage changes ($V_{Disturb}$) of 0.64%, 0.82%, and 0.77%, compared to 0.86%, 0.82%, and 0.68% using FS control.

Table VII shows that in Cases 1–3, a single-phase system using 2UPQC-2PV with PI control is able to maintain respectively load voltages (V_L) of 216.4 V, 223.7 V, and 216.0 V, while having similar load voltages with FS control of 216.3 V, 223.7 V, and 216.2 V. Table VII also shows that in Cases 1–3, a single-phase system using 2UPQC-2PV with PI control is capable of carrying I_L of 3.515 A, 3.635 A, and 3.508 A, respectively, whereas using FS control, similar I_L of 3.515 A, 3.634 A, and 3.512 A are achieved. The single-phase system using 2UPQC-2PV with PI control produces $V_{Disturb}$ of 1.64%, 1.68%, and 1.82% for Cases 1–3, respectively compared to 1.68%, 1.68%, and 1.73%, respectively with FS control.

TABLE VI
MAGNITUDE OF VOLTAGE AND CURRENT USING 1UPQC-1PV

Case	Source voltage V_S(V)	Load voltage V_L(V)	Source current I_S(A)	Load current I_L(A)	Series voltage V_{SE}(V)	Shunt current I_{SH}(A)	Load voltage disturb $V_{Disturb}$(%)
PI method							
1	113.6	218.6	3469	3.543	104.6	−24.14	0.64
2	321.3	221.8	3333	3.604	99.5	−23.54	0.82
3	66.62	218.3	6663	3.546	152.0	−22.91	0.77
Fuzzy-Sugeno method							
1	113.6	218.1	3469.	3.543	104.5	−23.14	0.86
2	321.3	221.8	3333	3.605	99.48	−23.54	0.82
3	66.61	218.5	6663	3.550	152.2	−22.90	0.68

TABLE VII
MAGNITUDE OF VOLTAGE AND CURRENT USING 2UPQC-2PV

Case	Source voltage V_S(V)	Load voltage V_L(V)	Source current I_S(A)	Load current I_L(A)	Series voltage V_{SE}(V)	Shunt current I_{SH}(A)	Load voltage disturb $V_{Disturb}$(%)
PI method							
1	113.4	216.4	3472	3.515	102.9	−15.30	1.64
2	321.3	223.7	3333	3.635	97.63	−15.82	1.68
3	66.6	216.0	6661	3.508	149.7	−15.12	1.82
Fuzzy-Sugeno method							
1	113.5	216.3	3472	3.514	102.9	−15.30	1.68
2	321.0	223.7	3333	3.634	97.64	−15.82	1.68
3	66.6	216.2	6661	3.512	149.8	−15.11	1.73

TABLE VIII
VOLTAGE AND CURRENT THD USING 1UPQC-1PV

Case	Source voltage V_S(V)	Load voltage V_L(V)	Source current I_S(A)	Load current I_L(A)	Series voltage V_{SE}(V)	Shunt current I_{SH}(A)
PI method						
1	0.17	0.97	1.08	1.11	3.36	0.47
2	0.01	0.85	0.09	0.81	3.45	0.35
3	0.10	3.61	0.08	3.62	5.46	4.51
FS method						
1	0.09	0.08	0.48	1.04	3.29	0.29
2	0.00	0.81	0.02	0.76	3.48	0.23
3	0.02	2.20	0.01	2.21	3.60	3.12

C. Analysis of Voltage and Current Harmonics

Figures 15 and 16 respectively show harmonic spectra of I_S, I_L, V_S and V_L in Case 1 (S-Sag-NL) and 2UPQC-2PV using dual-FS method.

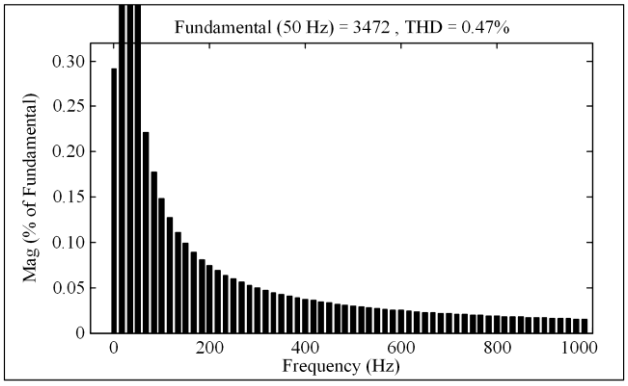

(a)

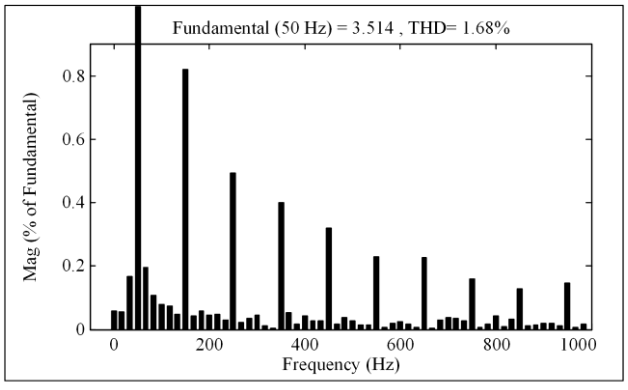

(b)

Fig. 15. Harmonic spectra. (a) I_S in Case 1 (S-Sag-NL) 2UPQC-2PV using dual-FS method. (b) I_L in Case 1 (S-Sag-NL) and 2UPQC-2PV using dual-FS method.

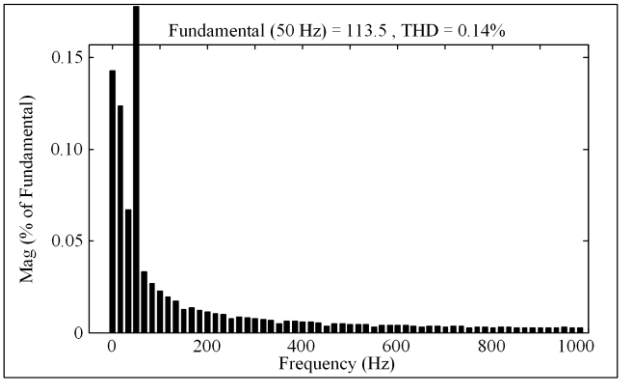

(a)

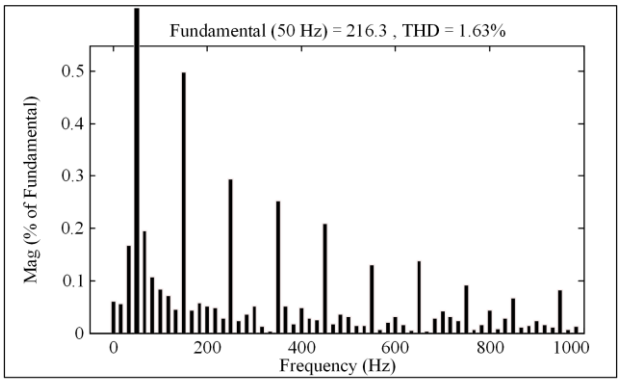

(b)

Fig. 16. Harmonic spectra. (a) V_S in Case 1 (S-Sag-NL) and 2UPQC-2PV using dual-FS method. (b) V_L in Case 1 (S-Sag-NL) and 2UPQC-2PV using dual-FS method.

Figure 15 shows that in Case 1, the 2UPQC-2PV configuration with the dual-FS method is capable of producing a source current THD of 0.47%, lower than the load current THD of 1.68%. The 2UPQC-2PV configuration with the dual-FS method is capable of

injecting a I_{SH} so that it can reduce the THD of the I_S according to the IEEE 519 standard. Figure 16 shows that in Case 1, the 2UPQC-2PV configuration with the dual-FS is able to produce a load voltage THD of 1.63%. Although it is higher than the source voltage THD of 0.14%, it meets the THD voltage limit of the IEEE-519 Standard. Using the same procedure, the THD values of V_S, V_{SE}, V_L, I_S, I_{SH} and I_L in the two UPQC-PV configurations, two control methods, and three cases are obtained, and the results are presented in Tables VIII and IX.

TABLE IX
VOLTAGE AND CURRENT THD USING 2UPQC-2PV

Case	Source voltage V_S(V)	Load voltage V_L(V)	Source current I_S(A)	Load current I_L(A)	Series voltage V_{SE}(V)	Shunt current I_{SH}(A)
Dual-PI method						
1	0.20	1.68	1.08	1.73	6.67	0.47
2	0.01	1.58	0.09	1.22	7.05	0.31
3	0.10	3.91	0.08	3.88	6.67	4.34
Dual-FS method						
1	0.14	1.63	0.47	1.68	6.65	0.34
2	0.00	1.55	0.01	1.19	7.09	0.23
3	0.03	2.71	0.01	2.65	5.29	2.98

Table VIII shows that the combination of 1UPQC-1PV with PI control for Cases 1–3 is capable of producing V_L THDs of 0.97%, 0.85%, and 3.61%, respectively. In the same configuration with FS control, the load voltage THDs are reduced to 0.08%, 0.81%, and 2.20% for Cases 1–3, respectively. In addition, the I_S THDs are 1.08%, 0.09%, and 0.08% for Cases 1–3, respectively. In comparison, using FS control, the I_S THDs are reduced to 0.48%, 0.02%, and 0.01% for Cases 1–3, respectively. Table VIII also shows that in the 1UPQC-1PV configuration with Cases 1–3, the PI and dual-FS controls are able to reduce the THD of the source current compared to the THD of the I_L.

Table IX shows that the combination of 2UPQC-2PV with dual-PI control, experiencing interference with Cases 1–3, is capable of producing V_L THDs of 1.68%, 1.58%, and 3.91%, respectively, whereas with dual-FS control, they are reduced to 1.63%, 1.55%, and 2.71% for Cases 1–3, respectively. The combination of 2UPQC-2PV with dual-PI control is capable of producing I_S of 1.08%, 0.09% and 0.08% for Cases 1–3, respectively, while using dual-FS control the corresponding THDs are reduced to 0.47%, 0.01%, and 0.01% for Cases 1-3, respectively. Table IX also shows that the 2UPQC-2PV configuration using the dual-PI and dual-FS controls is able to reduce the THD of the I_S compared to the THD of the I_L for Cases 1–3.

D. Analysis of PV Output and Load Active Power

PV output and load power using PI and FS methods for 1UPQC-1PV and 2UPQC-2PV configurations are shown in Tables X and XI, respectively.

TABLE X
PV OUTPUT AND LOAD POWER USING 1UPQC-1PV USING PI AND FS METHODS

Cases	PV1 voltage V_{PV1}(V)	DC1 voltage V_{DC1}(V)	PV1 current I_{PV1}(A)	PV1 power P_{PV1}(W)	DC1 power P_{DC1}(W)	Load power P_L(W)
PI method						
1	167.5	167.5	536.5	72 130	72 130	386.7
2	192.7	192.7	462.2	71 390	71 390	399.6
3	213.4	213.4	850.4	75 680	75 680	386.7
FS method						
1	177.2	177.2	445.4	7209.0	7209.0	386.7
2	162.8	162.8	489.3	71 350	71 350	399.5
3	164.0	164.0	518.3	75 390	75 390	386.8

Table X shows that the combination of 1UPQC-1PV and using PI and FS controls is able to produce the same V_{PV1} and V_{DC1}. I_{PV1} flowing into the DC-link circuit without a capacitor in the 1UPQC-1PV combination results in the same P_{PV1} and P_{DC1}. Case 3 in the combination of 1UPQC-1PV with PI and FS control shows that PV1 is able to inject the highest power (P_{PV1}) so that it is still able to distribute the P_L with a value close to those of Cases 1 and 2.

Table XI shows that the combination of 2UPQC-2PV and using dual-PI and dual-FS controls is capable of producing the same V_{PV1} and V_{PV2} with V_{DC1} and V_{DC2} The I_{PV1} and I_{PV2} flowing into DC-link 1 and DC-link 2 circuits without capacitors on the 2UPQC-2PV combination, lead to the same P_{PV1}, P_{PV2}, P_{DC1}, and P_{DC2}. Case 3, in the combination of 2UPQC-2PV with dual-PI and dual-FS controls, shows that PV1 and PV 2 are able to inject the largest output power of PV1 (P_{PV1}) and PV2 (P_{PV2}) so that they are still able to distribute P_L with a value close to those of Cases 1 and 2.

TABLE XI
PV OUTPUT AND LOAD POWER USING 2UPQC-2PV USING PI AND FS METHODS

Case	PV1, PV2 voltage V_{PV1}, V_{PV2} (V)	DC1, DC2 voltage V_{DC1}, V_{DC2} (V)	PV1, PV2 current I_{PV1}, I_{PV2} (A)	PV2 current I_{PV2} (A)	PV1, PV2 power P_{PV1}, P_{PV2} (W)	DC1, DC2 power P_{DC1}, P_{DC2} (W)	Load active power P_L (W)
Dual-PI Method							
1	209.3	209.3	239.3	239.3	72 760	72 760	380.4
2	192.3	192.3	236.8	236.8	73 250	73 250	406.3
3	187.3	187.3	132.2	132.2	75 110	75 110	378.5
Dual-FS Method							
1	176.4	176.4	530.9	530.9	72 750	72 750	380.5
2	171.6	171.6	454.4	454.4	72 410	72 410	406.2
3	203.7	203.7	562.9	562.9	75 790	75 790	378.6

E. Analysis of Load Voltage Changes, Load Voltage Harmonics, Source Current Harmonics, and Load Active Power

Figure 17 shows that in Cases 1–3 a single-phase system using the 2UPQC-2PV configuration with dual-PI and dual-FS controls produces a higher voltage change ($V_{Disturb}$ above 1.64%) than when using the 1UPQC-1PV configuration ($V_{Disturb}$ above 0.64%). The load voltage changes in all the scenarios are still within the limit of the maximum voltage change value ($V_{Disturb}$ under 5%).

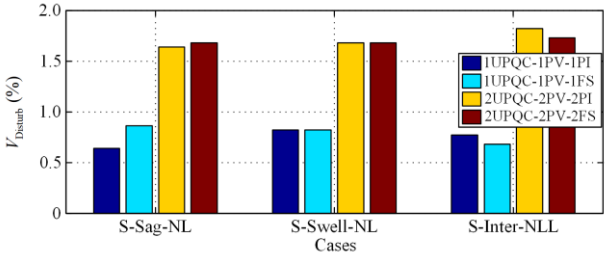

Fig. 17. Performance of changing load voltage ($V_{Disturb}$) in three disturbance cases.

Figure 18 shows that in Case 3, the 1UPQC-1PV and 2UPQC-2PV configurations with PI/dual-PI and FS/dual-FS control produce the highest load voltage THDs (above 2.20%) compared to those of Cases 1 and 2. The 1UPQC-1PV configuration in Cases 1–3 using PI and FS controls is capable of producing a lower THD load voltage than the 2UPQC-2PV configuration. In the 1UPQC-1PV configuration in the three disturbance Cases, the FS control is able to produce a lower load voltage THD than the PI control. In the 2UPQC-2PV configuration

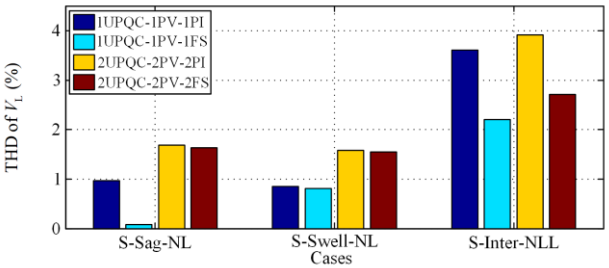

Fig. 18. Performance of load voltage (V_L) THD in three disturbance cases.

in the three disturbance cases, the dual-FS control is also able to produce a lower load voltage THD than the dual-PI control. In all the studied scenarios, the produced load voltage THDs are lower than the IEEE 519 limits.

Figure 19 shows that for Case 1, the 1UPQC-1PV and 2UPQC-2PV configurations with PI/dual-PI and FS/dual-FS controls produce higher source current THD (over 0.47%) than Cases 2 and 3. In Case 3, using configurations of 1UPQC-1PV and 2UPQC-2PV with PI/dual-PI and FS/dual-FS control produces the lowest source current THD (maximum THD of 0.08%) of the three cases. In the 1UPQC-1PV configuration with the three fault cases, the FS control is able to produce a lower source current THD than the PI control, whereas in the 2UPQC-2PV configuration the control produces a lower source current THD than the dual-PI control. The configurations of 1UPQC-1PV and 2UPQC-2PV with PI/dual-PI and FS/dual-FS control in the three disturbance cases are capable of generating sourcing current THD below the IEEE 519 limits.

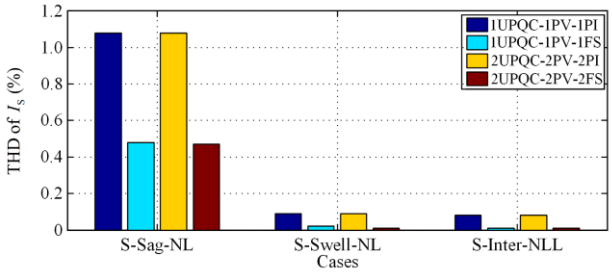

Fig. 19. Performance of source current (I_S) THD under in three disturbance cases.

Figure 20 shows that the 1UPQC-1PV and 2UPQC-2PV configurations with the PI/dual-PI and FS/dual-FS methods are capable of delivering the highest load active power (P_L above 399.5 W) in Case 2. In Case 3, the 1UPQC-1PV configuration using the FS method is capable of delivering active power (P_L of 386.8 W) close to that of Case 1 (P_L of 386.7 W). In Case 3, the 2UPQC-2PV configuration with dual-FS is also capable of delivering active power (P_L of 378.6 W) close to that of Case 1 (P_L of 380.5 W).

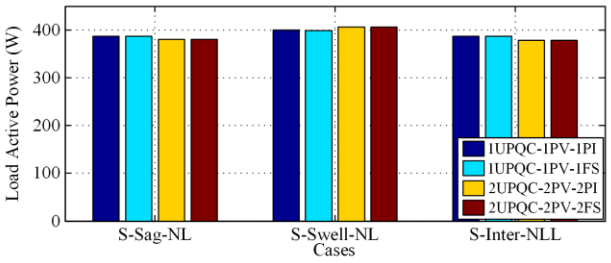

Fig. 20. Performance of load active power (P_L) in three disturbance cases.

F. System Validation and Comparison

Table XII shows the system validation results for the research compared to the previous nine studies. The observed parameters are the load voltage THD, source current THD, type of interference mitigation, PV-injected UPQC difference, and battery energy storage (BES). The three-phase UPQC configuration using the three-dimensional space vector PWM (3Ph-UPQC-3D-SVPWM) was implemented [17]. The types of disturbance that are mitigated are sag, imbalance, and NL which produce average V_L and I_S THDs of at least 1.43% and 3.37%, respectively. The UPQC system uses only a DC-link capacitor without PV injection and BES.

Reference [18] investigated 1PH-UPQC using a notch filter and feedback to suppress DC-link voltage ripple due to low frequency effects. The type of interference mitigated is limited to NL which produces an I_S THD of 1.32%. The UPQC system uses DC-link capacitors without PV injection and BES. In [19], a Ph-UPQC-Modular Multilevel Converter was implemented to mitigate PQ voltage sources and load currents. The types of disturbance mitigated are sag, swell, linear load (LL) and NL which produce a minimum average V_L and I_S THDs of 3.89% and 2.87%, respectively. The UPQC system uses only a DC-link capacitor. Reference [20] carried out a power flow analysis and increased PQ on the 3Ph-UPQC-PV-WT system. The types of interference mitigated are sag, imbalance and NL which produce average V_L and I_S THDs of at least 1.4% and 29%, respectively. The UPQC system uses a DC-link capacitor supplied by PV-WT.

The module for the AC microgrid (ACMG) as a 3-phase modulated-unified power quality conditioner (3PH-Modulated-UPQC) was proposed in [21]. The type of disturbance mitigated is only NL and produces minimum average V_L and I_S THDs of 4.4% and 5.3%, respectively. The UPQC system uses a DC-link capacitor and is supplied with PV-WT. The combination of 3Ph-UPQC-PV-WT connected to the 3P3W grid system to increase PQ was examined in [22]. The types of disturbance mitigated are sag and NL which produce a minimum average V_L and I_S THDs of 2.13 % and 5.27 %, respectively. The UPQC system uses DC-link capacitors and is supplied with PV-WT.

TABLE XII
PROPOSED RESEARCH OF SINGLE-PHASE 2UPQC-2PV WITHOUT DC-LINK CAPACITORS USING FS COMPARED WITH PREVIOUS RESEARCH

No.	Authors	Method	THD V_L(%)	THD I_S(%)	Disturbance mitigation	UPQC injected by PV	DC-link capacitor	BES
1.	Y. A. Garces-Gomez, et. al, 2019 [17]	3PH-UPQC-3D-SVPWM	1.43 (Average)	3.37 (Average)	Sag, Unbalance, NL	NA	A	NA
2.	L. Meng, et. al, 2021 [18]	1PH-UPQC-Low frequency DC-link Riple	NA	1.32	NL	NA	A	NA
3.	T. M.T Thentral, et. al., 2022 [19]	3PH-UPQC-modular-multilivel Converter	3.89 (Average)	2.87 (Average)	Sag, Swell, LL, NL	NA	A	NA
4.	N. Zanib, et, al, 2022 [20]	3PH-UPQC-PV-WT	1.4 (Average)	29 (Average)	Sag, Unbalance, NL	A and also with WT	A	NA
5.	N. Khosravi, 2022 [21]	3PH-modulated-UPQC	4.4	5.3	NL	NA	A	NA
6.	T. Lei, et. al, 2022 [22]	3PH-UPQC-PV-WT	2.13 (Average)	5.27 (Average)	Sag, NL	A and also with WT	A	NA
7.	K. Sarita, et. al, 2020 [23]	3PH-UPQC-PV-WT-EVA-FLC	6.27% (Average)	2.37% (Average)	Sag, Swell, LL, NL	A and also with wind turbine (WT)	A	A
8.	M.A. Mansoor, et. al, 2020 [24]	3PH-UPQC-PV-BES	0.28% (Average)	2.663% (Average)	Sag, Swell, NL	A	A	A
9.	G. M. Pelz, et. al., 2000 [25]	DG-UPQC-1PH-3Ph	1.167 (Average)	2.2	NL	A	A	NA
10.	**Proposed research**	**1PH-2UPQC-2 PV-2FS**	**1.55**	**0.01**	**Sag, swell, interruption, NL**	**A**	**NA**	**NA**

Note: A = Available; NA = Not Available; LL = Linear Load; NL = Non-Linear Load

Reference [23] observed an increase in power quality using 3PH-UPQC-PV-WE-EVA-FLC. The types of disturbance mitigated are sag, swell, LL, and NL which produce a minimum average V_L and I_S THDs of 6.27% and 2.37%, respectively. The UPQC system uses a DC-link capacitor, PV-WT injection, and BES. In [24],

power quality problems in the grid and harmonics due to NL were investigated using 3PH-UPQC-PV-BES. The types of disturbance mitigated are sag, swell and NL which produce a minimum average V_L and I_S THDs of 0.28% and 2.663%, respectively. The UPQC system uses a DC-link capacitor, PV-WT injection, and BES. Reference [25] implemented a DG-UPQC-1PH-3PH system using PV to serve local loads connected to a 3P3W system and serve rural and/or remote area customers supplied by a single-phase network. The type of disturbance that is mitigated is only NL which produces a minimum average V_L and I_S THDs of 1.67% and 2.2%, respectively. The UPQC system uses a DC-link capacitor supplied by PV.

This paper has proposed the 1Ph-2UPQC-2PV-2FS system for mitigating power quality issues on the source and load sides. The types of disturbance mitigated are sag, swell, interruption, and NL resulting in a minimum V_L and I_S THDs of 1.55% and 0.01%, respectively (see Table XII). The THD of V_L in the proposed system is slightly higher that than in [17], but the THD of I_S is lower than that in [18], while both meet the IEEE-519 limits. The system provides the best performance because it is also able to mitigate disturbances to interruption voltage, compared to [19], [23], [24]. The UPQC system also has better circuit efficiency because it only uses PV injection without a DC-link capacitor and BES compared to [23], [24].

IV. Conclusion

The 2UPQC-2PV configuration to improve power quality performance in a single-phase 220 V / 50 Hz distribution system has been implemented together with the 1UPQC-1PV configuration. The 2UPQC-2PV configuration is proposed to anticipate the failure of the two inverters in one of the UPQC circuits. The proposed model does not use a DC-link capacitor whose role is replaced by a PV generator to keep the UPQC DC voltage constant, while at the same time supplying power to the load during interruptions. The dual-FS method is used to overcome the weakness of the dual-PI control in determining the optimum parameters of proportional and integral constants. Disturbance simulations are carried out for the 2UPQC-2PV and 1UPQC-1PV configurations using dual-FS and dual-PI controls, and three cases, i.e., Case 1 (S-Sag-NL), Case 2 (S-Swell-NL), Case 3 (S -Inter-NL).

In the three disturbance cases, the 2UPQC-2PV configuration with dual-PI and dual-FS controls produces a higher voltage change ($V_{Disturb}$ above 1.64%) than the 1UPQC-1PV configuration ($V_{Disturb}$ above 0.64%). For both 1UPQC-1PV and 2UPQC-2PV in the three disturbance cases, the FS/dual-FS control is able to produce a lower load voltage and source current THDs than the PI/dual-PI control, while meeting the IEEE 519 standard (see Figs. 18 and 19). 1UPQC-1PV and 2UPQC-2PV using the PI/dual-PI and FS/dual-FS methods with Case 2 are capable of delivering the highest load active power (P_L above 399.5 W). In Case 3, the 2UPQC-2PV configuration using the dual-FS method is able to distribute P_L of 378.6 W which is close to that in Case 1, i.e. 380.5 W.

The cost for the 2UPQC-2PV is higher than that of the 1UPQC-1PV. Thus, even though 2UPQC-2PV is able to provide better technical performance, the economic aspect needs to be considered.

The source voltages in Case 3 are still over 0.1 p.u. limit of the IEEE standard 1159-1995 interruption voltage during the disturbance (0.15 s–0.35 s) [36]. This situation exists because, despite the source voltage been short-circuited to zero, the PV is still injecting electricity through the Se-AF and the series transformer. To remedy this issue, future studies on the Se-AF may be suggested using series voltage intelligent control.

Acknowledgements

The authors would like to acknowledge the Directorate of Research, Technology and Society Services-Ministry of Education, Culture, Research and Technology of the Republic of Indonesia for funding this research in the scheme of National Competitive Fundamental Research 1st year.

Authors' Contributions

Amirullah Amirullah and Adiananda Adiananda: conceptualization, methodology, software, formal analysis, investigation, data curation, writing – original draft. Amirullah Amirullah: validation, resources, writing – review and editing, visualization, supervision. Both authors read and approved the final manuscript.

Funding

This research is supported by the Directorate of Research, Technology and Community Service- Ministry of Education, Culture, Research, and Technology, the Republic of Indonesia in the scheme of National Competitive-Fundamental Research 1st year [Decree Letter Number 033/E5/PG.02.00/2022 on 27 April 2022 and Agreement/Contract Number Master Contact Number 159/E5/P6.02.00.PT/2022 on 10 May 2022 and Derivative Contract Number 009/SP2H/PT/LL7/2022 on 10 Mei 2022 and Number 001/VI/2022/LPPM/UBHARA on 10 May 2022.

Availability of Data and Materials

Not applicable.

DECLARATIONS

Competing interests: The authors declare that they have no known competing financial interests or personal relationships that could have appeared to influence the work reported in this paper.

AUTHORS' INFORMATION

Amirullah Amirullah received bachelor's and master's degrees in electrical engineering from the University of Brawijaya Malang and Institut Teknologi Sepuluh Nopember (ITS) Surabaya, in 2000 and 2008, respectively. And he received the doctoral degree in electrical engineering in Power System and Simulation Laboratory (PSSL) ITS Surabaya. From 2002 until now, he has been working as a lecturer and assistant professor at the Universitas Bhayangkara Surabaya. His research interest includes power distribution/electronics modelling and simulation, power quality, harmonics mitigation, design of filter/power factor correction, renewable energy-based PV/wind turbine and artificially intelligent system.

Adiananda Adiananda received bachelor and master degree in electrical engineering from University of Bhayangkara Surabaya and master of computer science from Gadjah Mada University (UGM) Yokyakarta, in 1996 and 2016, respectively. Since 1998, He had been working as a lecturer in University of Bhayangkara Surabaya. He is interested in research of application of artificial intelligent in modelling power electronics and computer system.

REFERENCES

[1] B. Han, B. Bae, and H. Kim et al., "Combined operation of unified power-quality conditioner with distributed generation," *IEEE Transactions on Power Delivery,* vol. 21, no. 1, pp. 330-338, Jan, 2006.

[2] V. Khadkikar, "Enhancing electric power quality using UPQC: a comprehensive overview," *IEEE Transactions on Power Electronics*, vol. 27, no. 5, pp. 2284-2297, May 2012.

[3] V. F. Pires, D. Foito, and A. Cordeiro *et al*. (2017, Jun.). "PV generators combined with UPQC based on a dual c onverter structure," Presented at IEEE 26th International Symposium on Industrial Electronics (ISIE). [Online].Av ailable: https://ieeexplore.ieee.org/document/8001518.

[4] R. J. M. dos Santos, J. C. da Cunha, and M. Mezaroba, "A simplified control technique for a dual unified power quality conditioner," *IEEE Transactions on Industrial Electronics*, vol. 61, no. 11, pp. 5851-5860, Nov. 2014.

[5] B. W. França, L. F. da Silva and M. Aredes, "Comparison between alpha-beta and DQ-PI controller applied to IUPQC operation," in *XI Brazilian Power Electronics Conference*, Natal, Brazil, Sept. 2011, pp. 306-311.

[6] B. W. França and M. Aredes, "Comparisons between the UPQC and its dual topology (iUPQC) in dynamic response and steady-state,"*in IECON 2011-37th Annual Conference of the IEEE Industrial Electronics Society,* Melbourne, VIC, Australia, Nov. 2011, pp. 1232-1237.

[7] B. W. Franca, L. F. da Silva, and M. A. Aredes, "An improved iUPQC controller to provide additional grid-voltage regulation as a STATCOM," *IEEE Transactions on Industrial Electronics.* Vol. 62, no. 3, pp. 1345-1352, Mar. 2015.

[8] S. A. O. da Silva, L. B. G. Campanhol, and G. M. Pelz *et al*., "Comparative performance analysis involving a three-phase UPQC operating with conventional and dual/inverted power-line conditioning strategies," *IEEE Transactions on Power Electronics,* vol. 35, no. 11, pp. 11652-11665, Nov. 2020.

[9] N. S. Borse and S. M. Shembekar, "Power quality improvement using dual topology of UPQC," *in 2016 International Conference on Global Trends in Signal Processing, Information Computing and Communication (ICGTSPICC)*, Jalgaon, India, Dec. 2016, pp. 428-431.

[10] R. A. Modesto, S. A. O. da Silva, and A. A. de Oliveira Júnior. "Power quality improvement using a dual unified power quality conditioner/uninterruptible power supply in three-phase four-wire systems," *IET Power Electronics*, vol. 8, no. 9, pp. 1595-1605, Sept. 2015.

[11] R. A. Modesto, S. A. O. da Silva, and A. A. de Oliveira *et al*., "Versatile unified power quality conditioner applied to three-phase four-wire distribution systems using a dual control strategy," *IEEE Transactions on Power Electronics*, vol. 31, no. 8, pp. 5503-5514, Aug. 2016.

[12] S. M. Fagundes and M. Mezaroba, "Reactive power flow control of a Dual Unified Power Quality Conditioner," in *IECON 2016-42nd Annual Conference of the IEEE Industrial Electronics Society*, Florence, Italy, Oct. 2016, pp. 1156-1161.

[13] S. M. Fagundes, F. L. Cardoso, and E.V. Stangler *et al*., "A detailed power flow analysis of the dual unified power quality conditioner (iUPQC) using power angle control (PAC)," *Electric Power Systems Research*, vol. 192, Mar. 2021.

[14] S. Paithankar and R. Zende, "Comparison between UPQC, iUPQC and improved iUPQC," in *2017 Third International Conference on Sensing, Signal Processing and Security (ICSSS)*, Chennai, India, May 2017, pp. 61-64.

[15] G. Mythily and S. V. R. Lakshmi Kumari, "Power quality improvement by IUPQC," in *International Conference on Inventive Research in Computing Applications, (ICIRCA),* Chennai, India, Jul. 2018. pp. 1280-1285.

[16] S. P. Thota and S. K. Peddapelli, "Fuzzy controller based interline unified power quality conditioner (IUPQC) in multi-feeder systems," in *International Conference on Engineering, Science, and Industrial Applications (ICESI),* Tokyo, Japan, Aug. 2019, pp. 1-5.

[17] Y. A. Garces-Gomez, F. E. Hoyos, and J. E. Candelo-Becerra, "Classic discrete control technique and 3D-SVPWM applied to a dual unified power quality conditioner," *Applied Sciences-Basel,* vol. 9, no. 23, Dec. 2019.

[18] L. Meng, L. Ma, and W. Zhu *et al*., "Control strategy of single-phase UPQC for suppressing the influences of low-frequency DC-link voltage ripple," *IEEE Transactions on Power Electronics*, vol. 37, no. 2, pp. 2113-2124, Feb. 2022.

[19] T. M. Thamizh Thentral, R. Palanisamy, and S. Usha *et al*., "The improved unified power quality conditioner with the modular multilevel converter for power quality improvement," *International Transactions on Electrical Energy Systems*, Sept. 2022.

[20] N. Zanib, M. Batool, and S. Riaz *et al*., "Analysis and power quality improvement in hybrid distributed generation system with utilization of unified power quality conditioner," *CMES-Computer Modeling in Engineering and Sciences,* vol. 134, no. 2, pp. 1105-1136, 2022.

[21] N. Khosravi, A. Abdolvand, and A. Oubelaid *et al*., "Improvement of power quality parameters using modulated unified power quality conditioner and switched inductor boost converter by the optimization techniques for a hybrid AC/DC microgrid," *Scientific Reports,* vol. 12, no. 1, Dec. 2022.

[22] T. Lei, S. Riaz, and N. Zanib *et al*., "Performance analysis of grid-connected distributed generation system integrating a hybrid wind-PV farm using UPQC," *Complexity*, Mar. 2022.

[23] K. Sarita, S. Kumar, and A.S.S. Vardhan *et al*., "Power enhancement with grid stabilization of renewable energy-based generation system using UPQC-FLC-EVA Technique," *IEEE Access.* Vol. 8, pp. 207443-207464, 2020.

[24] M. A. Mansor, K. Hasan, and M.M. Othman, *et al*., "Construction and performance investigation of three-phase solar PV and battery energy storage system integrated UPQC," *IEEE Access,* Vol. 8, pp. 103511-103538, 2020.

[25] G.M. Pelz, S.A.O. da Silva, and L.P. Sampaio, "Distributed generation integrating a photovoltaic-based system with a single-to three-phase UPQC applied to rural or remote areas supplied by single-phase electrical power," *Electrical Power and Energy Systems,* vol. 117, May. 2020.

[26] A. Soeprijanto and O. Penangsang, "Power transfer analysis using UPQC-PV system under sag and interruption with variable irradiance," in *2020 International Conference on Smart Technology and Applications (ICoSTA)*, Surabaya, Indonesia, Feb. 2020.

[27] L. B. G. Campanhol, S. A. O. da Silva and A. O. Azauri. "A three-phase four-wire grid-connected photovoltaic system using a dual unified power quality conditioner," in *2015 IEEE 13th Brazilian Power Electronics Conference and 1st Southern Power Electronics Conference (COBEP/SPEC)*, Fortaleza, Brazil, Nov. 2015, pp. 1-6.

[28] A. A. Al-Shamma'a and K. E. Addoweesh, "Dual unified power quality conditioner based on open-winding transformers and series converters for grid-connected PV system," in *2017 9th IEEE-GCC Conference and Exhibition (GCCCE)*, Manama, Bahrain, May 2017, pp. 1-6.

[29] Amirullah, Adiananda, O. Penangsang, and A. Soeprijanto. "A dual UPQC to mitigate sag/swell, interruption, and harmonics on three phase low voltage distribution system," in *2020 Third International Conference on Vocational Education and Electrical Engineering (ICVEE)*, Surabaya, Indonesia, Oct. 2020, pp. 1-6.

[30] A. Amirullah, A. Adiananda, and O. Penangsang *et al*.,"Enhancing the performance of load real power flow using dual UPQC-dual PV system based on dual fuzzy Sugeno method," *International Journal on Electrical Engineering and Informatics,* vol. 13, no. 1, pp. 21-57, Mar. 2021.

[31] Y.A. Setiawan and A. Amirullah, "Implementation of single-phase DVR-BES based on unit vector template generation (UVTG) to mitigate voltage sag using arduino-uno and monitored in real-time through LabVIEW simulation," *International Journal of Intelligent Engineering and Systems,* vol. 14, no. 3, pp. 82-96, Jun. 2021.

[32] M.Y Lada, O. Mohindo, and A. Khamis *et al*., "Simulation single phase shunt active filter based on p-q technique using MATLAB/Simulink development tools environment," in *2011 IEEE Applied Power Electronics Colloquium (IAPEC)*, Johor Bahru, Malaysia, Apr. 2011, pp. 159-164.

[33] M. Hembram and A.K. Tudu, "Mitigation of power quality problems using unified power quality conditioner (UPQC)," in *Proceedings of the 2015 Third International Conference on Computer, Communication, Control and Information Technology (C3IT)*, Hooghly, India, Apr. 2015, pp. 1-5.

[34] A. Kiswantono, E. Prasetyo, and A. Amirullah, "Comparative performance of mitigation voltage sag/swell and harmonics using DVR-BES-PV system with MPPT-Fuzzy Mamdani/MPPT-Fuzzy Sugeno," *International Journal of Intelligent Engineering and Systems,* vol. 12, no. 2, pp. 222-235, Feb. 2019.

[35] A. Amirullah, A. Adiananda, and O. Penangsang *et al*., "Load active power transfer enhancement using UPQC-PV-BES system with fuzzy logic controller," *International Journal of Intelligent Engineering and Systems.* vol. 13, no. 2, pp. 329-349, Feb. 2020.